NUREG/CR-2264
PNL-4215

Characterization Methods for Ultrasonic Test Systems

Prepared by L. J. Busse, F. L. Becker, R. E. Bowey,
S. R. Doctor, R. P. Gribble, G. J. Posakony

Pacific Northwest Laboratory
Operated by
Battelle Memorial Institute

Prepared for
U.S. Nuclear Regulatory
Commission

Available from

GPO Sales Program
Division of Technical Information and Document Control
U. S. Nuclear Regulatory Commission
Washington, D. C. 20555

Printed copy price: $5.00

and

National Technical Information Service
Springfield, Virginia 22161

NUREG/CR-2264
PNL-4215
R5

Characterization Methods for Ultrasonic Test Systems

Manuscript Completed: April 1982
Date Published: July 1982

Prepared by
L. J. Busse, F. L. Becker, R. E. Bowey,
S. R. Doctor, R. P. Gribble, G. J. Posakony

Pacific Northwest Laboratory
Richland, WA 99352

Prepared for
Division of Engineering Technology
Office of Nuclear Regulatory Research
U.S. Nuclear Regulatory Commission
Washington, D.C. 20555
NRC FIN B2289

CHARACTERIZATION METHODS FOR ULTRASONIC TEST SYSTEMS

ABSTRACT

Methods for the characterization of ultrasonic transducers (search units) and instruments are presented. The instrument system is considered as three separate components consisting of a transducer, a receiver-display, and a pulser. The operation of each component is assessed independently. The methods presented were chosen because they provide the greatest amount of information about component operation and were not chosen based upon such conditions as cost, ease of operation, field implementation, etc. The results of evaluating a number of commercially available ultrasonic test instruments are presented.

SUMMARY

A common goal of those working in the area of ultrasonic testing is the development of effective and reproducible test results. To meet this goal, ultrasonic instrument operation must be repeatable and predictable. This document presents a series of measurement techniques that are being used at Pacific Northwest Laboratory (PNL) to quantify the performance of ultrasonic test instruments. The purpose of these techniques is to provide the greatest amount of information about the operating characteristics of the individual components that make up an ultrasonic test instrument.

Ultrasonic test instruments are considered as three subsystems: a transducer or search unit, a receiver-display, and a pulser. The performance of each subsystem is assessed independently. The measurement procedures described allow the following properties to be determined:

1. Transducer
   - acoustic frequency response (spectrum)
   - efficiency (insertion loss or pulse echo sensitivity)
   - time domain response
   - electrical impedance
   - sound field patterns
2. Receiver-Display
   - frequency response (bandwidth)
   - amplitude response (linearity)
   - noise (referred to input)
   - input sensitivity
3. Pulser
   - time domain response
   - frequency response
   - output impedance

Measurement procedures have been demonstrated on commercially available transducers and test instruments. A discussion of the results is presented as well as some general suggestions for improvement of instrument performance.

CONTENTS

LIST OF FIGURES

LIST OF FIGURES

(cont'd)

CHARACTERIZATION METHODS FOR ULTRASONIC TEST SYSTEMS

1.0 INTRODUCTION

The need for standardized and reproducible ultrasonic test instrument performance underlies all efforts aimed toward developing reproducible test procedures (Sachse and Hsu 1979; O'Donnell, Busse and Miller, 1980; Lidington and Silk 1972; Papadakis 1977). Here "reproducible" means that results obtained with the instrument must be repeatable from day to day at a given location and also that test procedures can be reproduced at many locations by different personnel. This report presents methods designed to measure the operational characteristics of ultrasonic test instruments. These methods are based largely on automated (i.e., computerized) procedures so that large amounts of data can be accumulated and handled conveniently using a laboratory analysis system. These methods were implemented at Pacific Northwest Laboratory (PNL) to help document the performance characteristics of typical inspection units currently being used in industry. This work supports the program, "Integration of NDE Reliability and Fracture Mechanics," which is sponsored by the Nuclear Regulatory Commission. The NRC program was established to determine the reliability of current in-service inspection (ISI) techniques and to develop recommendations that will assure a suitably high inspection reliability. From the basic knowledge of the operational characteristics of available ultrasonic test equipment, improved test procedures and equipment specifications can be developed.

Ultrasonic test instruments can be divided into three major subsystems: 1) the transducer, 2) the receiver-display, and 3) the pulser. The characterization methods presented in this document use linear circuit theory to characterize these subsystems individually.

The ultrasonic transducer and a fixed length of coaxial cable are considered here as a single functional unit. The transducer unit is characterized under experimental conditions closely related to the actual operating conditions of the transducers, e.g., transient pulse excitation and proper mechanical (i.e., acoustic) loading of the transducer front surface. The transducer properties which are measured include the complex electrical impedance of the device, the insertion loss, the relative pulse echo sensitivity, and the bandwidth and center frequency of the unit. The sound field produced by these transducers is also mapped.

The measured properties of the receiver-display subsystem are bandwidth, linearity, input noise and input sensitivity. These properties of the receiver-display may vary as the sensitivity, rf filtering and video filtering of the instrument are varied. Because of the many possible combinations of tunings and adjustments, the receivers are characterized at a limited number of settings. Receiver-display systems with analog outputs that are normally used to drive strip chart recorders can be characterized using an automated measurement system. If no analog outputs are provided, a semiautomated measurement system can be used to record the video display of the instrument. With these two measurement systems it is also possible to compare the video display output with the analog or chart recorder output. In this way, problems with the recorder system can be identified.

The pulser or transmitter subsystem is the most nonlinear component in the ultrasonic test instrument. For this reason, pulser characterization is limited. The pulser properties measured include the frequency spectrum of the high-voltage pulse under different electrical loading conditions and an estimate of the output impedance of the pulser circuit.

The results of experimental measurements made for several commercially available ultrasonic test instruments and transducers are presented as demonstrations of the testing methods. The results show the utility of the methods proposed for evaluating ultrasonic test systems and also give some insight into the variability found in present test equipment.

The following three sections (2.0, 3.0, 4.0) describe the test methods and demonstration results for the transducer, receiver-display, and pulser subsystems, respectively. A final section, Section 5.0, discusses the measurements needed to evaluate ultrasonic test system performance.

2.0 TRANSDUCER CHARACTERIZATION

The theory and measurement procedure for evaluating the electrical, electromechanical, and mechanical performance of transducers are presented. The methods used for electrical and electro-mechanical transducer evaluation are based on transient electrical excitation of the transducer. Spectrum analysis and application of linear circuit theory then allows the performance parameters, such as complex impedance, insertion loss, bandwidth, and bandwidth center frequency to be measured. The methods presented are generally applicable and can be used to evaluate the performance of many different designs of ultrasonic transducers, i.e., immersion or contact (both angled and normal beam) units. Care must be taken, however, when evaluating these different transducers. For example, it is important to maintain the proper mechanical loading of the transducers--immersion transducers must be evaluated in water; contact transducers must be coupled to metal; and angled beam transducers must be operated into a plastic wedge material. Experimental results are presented from transducers of different electrical, mechanical, and acoustic design.

The mechanical evaluation of the transducer is accomplished by mapping the sound field produced by the device. This evaluation is straightforward for immersion transducers (Posakony 1975). A technique is presented for direct mapping of the sound field produced by angled beam transducers in metal (Wuestenberg 1970, 1979).

2.1 MEASUREMENT THEORY

The measurement procedure presented is based on linear transfer functions (Sittig 1967; Sachse and Hsu 1979). Application of linear theory to transducer operation requires simplifying assumptions. First, the analysis is restricted

to a single mode of operation. In other words, a transducer designed to launch and receive longitudinal elastic waves will not transmit or respond to any other type of elastic wave. Second, a linear system response is assumed. Electrical and acoustic excitation levels are assumed to be small enough that they can be adequately described by linear equations of motion. The assumption of "small signal" response is not overly restrictive and is, in fact, the normal mode of operation for ultrasonic transducers.

2.1.1 Electrical Characterization

The recommended practice for characterization of the electrical properties of transducers requires that the complex electrical impedance (resistive and reactive components) of the device be measured (ASA 1970). For this measurement, both the voltage and current magnitudes and phases must be measured as a function of frequency. This measurement is generally carried out using a continuous-wave measurement instrument such as a vector impedance bridge. It is also possible to make a similar determination using transient voltage excitation and signal processing techniques (Sachse). Figure 1 describes the two-step measurement process for determining the complex impedance of an unknown load, $\tilde{Z}_\ell$.

In Step 1 the transient voltage, $v_1(t)$, is recorded by means of a transient waveform recorder or sampling scope. From this time domain signal, the complex Fourier transform is calculated:

$$\tilde{V}_1(\omega) = \int_{-\infty}^{\infty} v_1(t) e^{j\omega t} dt. \qquad (1)$$

In practice, this Fourier transformation is performed using a Fast Fourier Transform subroutine in a microcomputer. In the

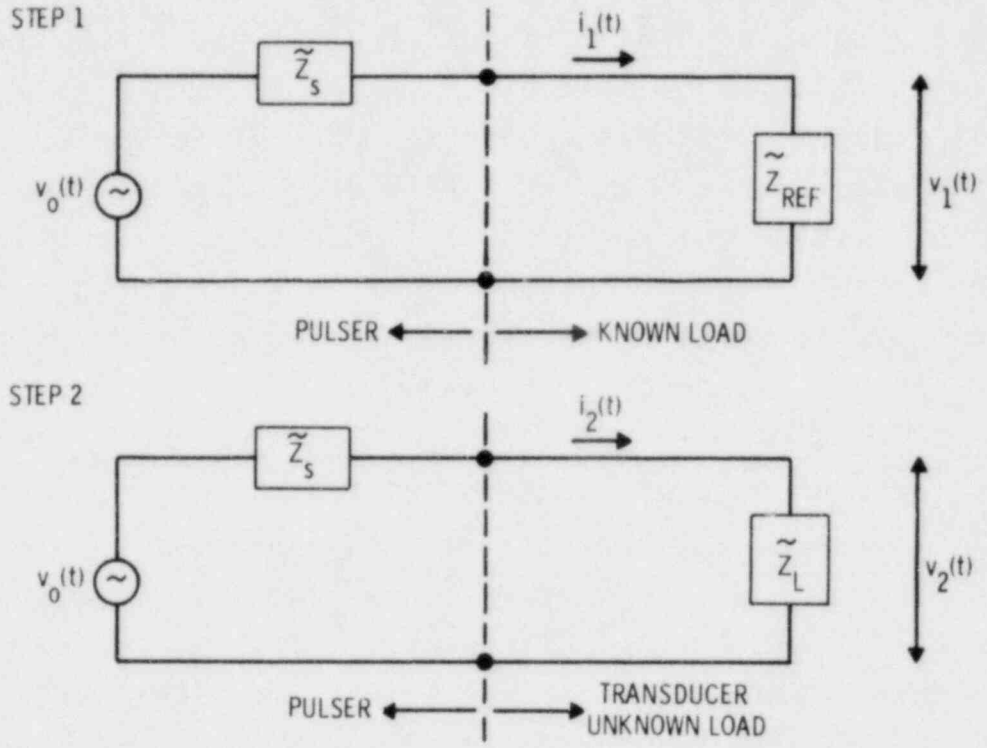

Figure 1. Equivalent Circuit Used to Measure the Complex Impedance of a Transducer

following equations the convention is that all capitalized variables are complex (have real and imaginary parts) and are functions of frequency. The voltage divider formed by Z_{REF} and Z_S allows the calculation of V_o:

$$V_o = \frac{Z_{REF} + Z_S}{Z_{REF}} V_1 \qquad (2)$$

A signal generator with a known output impedance [Z_S = (50 + j0) ohms] and a known reference load [Z_{REF} = (50 + j0) ohms] is used, so

$$V_o = 2V_1 \qquad (3)$$

Step 2 again involves recording a transient voltage, $\upsilon_2(t)$, where now the reference load has been replaced with the unknown electrical load, Z_L. This unknown load represents the ultrasonic transducer and an appropriate length of coaxial cable. The Fourier transform of $\upsilon_2(t)$ is again related to $\upsilon_o(t)$ by the voltage divider:

$$V_2 = \frac{Z_L}{Z_S + Z_L} V_o = \frac{2Z_L V_1}{Z_S + Z_L} \tag{4}$$

Now, calculating Z_L is a matter of algebra:

$$Z_L = \frac{V_2}{(2V_1 - V_2)} Z_S \tag{5}$$

For this method to work properly, some care must be exercised in the choice of the transient waveform $\upsilon_o(t)$. The magnitude of the transform pair of this signal ($|V_o|$) should have reasonable amplitude over the entire frequency range of interest. A square wave pulse of duration τ, where τ is less than one over the maximum frequency of interest, is sufficient for this purpose. The maximum frequency of interest is generally greater than twice the center frequency of the transducer.

Once the complex electrical impedance of the load has been determined, it is possible to calculate other useful electrical parameters such as the electrical power delivered to the transducer, P_T:

$$P_T = \frac{1}{2} \mathrm{Re}[I_2^* \times V_2] = \mathrm{Re}[Z_L] \frac{|V_2|^2}{2|Z_L|^2} \tag{6}$$

Here "Re" refers to taking the real part of the quantity in brackets.

2.1.2 Electromechanical Transducer Characterization

Electromechanical efficiency refers to the efficiency of the transducer for converting electrical to mechanical energy and the inverse process.

It is generally accepted that piezoelectric transducers operating into a fluid medium are reciprocal devices. The term reciprocal has many interpretations (Foldy and Prinakoff 1945; Primakoff and Foldy 1947; MacLean 1940; Carstensen 1947; Sabin 1964; Reid 1974); however, here the limited statement of reciprocity--the efficiency of the piezoelectric element as a transmitter is equal to the efficiency of the device as a receiver--is assumed.

Measurement of insertion loss combined with assumptions of reciprocity provides a means for determining the electromechanical efficiency of a transducer. The two-way insertion loss is defined as the ratio of the available electrical power generated by the transducer as a receiver to the electrical power dissipated in the device as a transmitter. The acoustic wave produced in the transmit mode is assumed to propagate without loss, reflect from a perfectly reflecting interface, and be received by the same transducer.

As seen in Section 2.1.1, Equation (6), knowledge of the complex impedance, Z_L, of the transducer and the complex spectra of the transmit waveform V_2 allows the calculation of P_T, the electrical power dissipated in the transducer in the transmit mode. Now consider the receive mode, described in Figure 2. Operating as a receiver, the piezoelectric action of the crystal can be represented as a voltage source in series with Z_L, the complex impedance of the transducer. This simple circuit must now drive the load presented to it by the pulser circuit (in this example, a 50-ohm resistive load). By Fourier transforming the observed voltage waveform

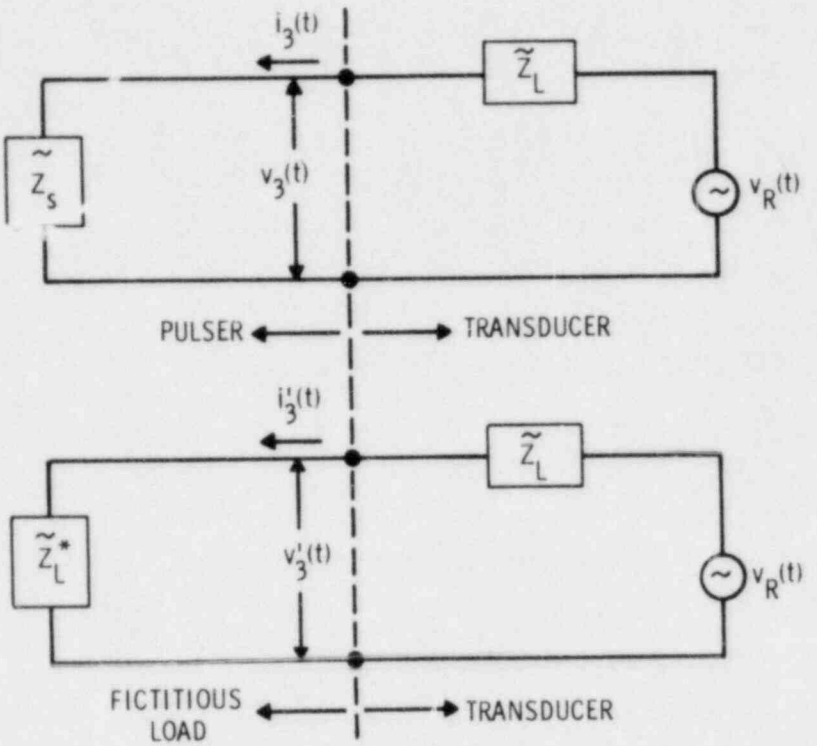

Figure 2. Equivalent Circuit Used to Evaluate the Efficiency of the Transducer Acting as a Receiver

$v_3(t)$, the observed power delivered to the load in the receive mode can be calculated.

$$P_R = \frac{1}{2} \mathrm{Re}[I_3^* V_3] = \mathrm{Re}[Z_S] \frac{|V_3|^2}{2|Z_S|^2} \tag{7}$$

The observed insertion loss is then simply the ratio of P_R to P_T. Similarly, the spectrum of the equivalent source voltage can be determined:

$$V_R = (1 + \frac{Z_L}{Z_S}) V_3 \tag{8}$$

In order to determine the ideal insertion loss, the available power generated by the transducer must be calculated. The

available power is the power which the transducer would deliver to a matched load. This is shown in Figure 2B as a fictitious matched Z_L^*, the complex conjugate of Z_L. Under these optimum loading conditions, the "observed" voltage can be predicted:

$$V_3' = \frac{Z_L}{Z_L + Z_L^*} V_R = \frac{Z_L}{2Re(Z_L)} V_R \qquad (9)$$

Substituting the previous expression for V_R,

$$V_3' = \frac{Z_L^* (Z_S + Z_L)}{2Z_S \, Re[Z_L]} V_3 \qquad (10)$$

The power available to Z_L is then

$$P_R' = \frac{1}{2} Re[I_3'^* \times V_3'] = \frac{1}{2} Re \frac{|V_3'|^2}{Z_L} \qquad (11)$$

Upon substitution of Equation (10) into (11):

$$P_R' = P_R \frac{(Z_L^* + Z_S)(Z_L + Z_S)}{(Z_L + Z_L^*)(Z_S + Z_S^*)} \qquad (12)$$

In other words, the available power P_R' can be calculated from the measured power P_R if Z_L, the impedance of the transducer, is known. The available power is equal to the measured power when the transducer impedance equals the output impedance, Z_S, of the pulser circuit.

It is now possible to evaluate the ideal insertion loss and hence the electromechanical efficiency, η, of the transducer.

$$\text{Insertion Loss} = \eta^2 = \frac{P_R'}{P_T} \qquad (13)$$

where P_T is defined by Equation (6) and P_R' is defined by Equation (12). For some transducers, it is difficult to

determine ideal insertion loss because of numerical anomalies which occur in the calculation of P_R'. In these situations, the simple ratio of P_R to P_T must be used.

Other means for characterizing the efficiency have been proposed. For example, in a swept frequency sinusoidal measurement (Erikson 1979) the relative loop sensitivity of the transducer has been defined as the ratio of the observed receive voltage to the loaded transmitter voltage at the center frequency of the transducer. The information needed for calculating relative loop sensitivity (and other indices of transducer performance) are present in the proposed transient calibration technique and can be extracted with appropriate algebraic manipulation.

For example, the loaded transmitter voltage V_T^L can be calculated from the ratio of the power spectral amplitudes of V_2 and V_1.

$$|V_T^L| = |V_2|/|V_1| \qquad (14)$$

This normalization is necessary to simulate an unload transmitter drive voltage that is frequency independent. The relative pulse echo sensitivity, expressed in dB, is then just

$$20 \log \left(\frac{|V_3|}{|V_2|}\right) \qquad (15)$$

The value of S_{rel} is established at the bandwidth center frequency.

The pulse echo sensitivity calculated in this way is a function of the ultrasonic frequency, and so measurement of useful transducer bandwidth, center frequency, and other performance parameters can be based on this curve.

2.2 MEASUREMENT PROCEDURE

The basic block diagram of the system used to gather the necessary data for transducer characterization is shown in Figure 3. The pulser used at PNL consists of a pulse generator capable of producing a 50-volt pulse across a 50-ohm load. A transient recorder with a high-impedance active probe is used to record the transient waveforms, and a microcomputer is used for control and the signal processing functions described in the previous section.

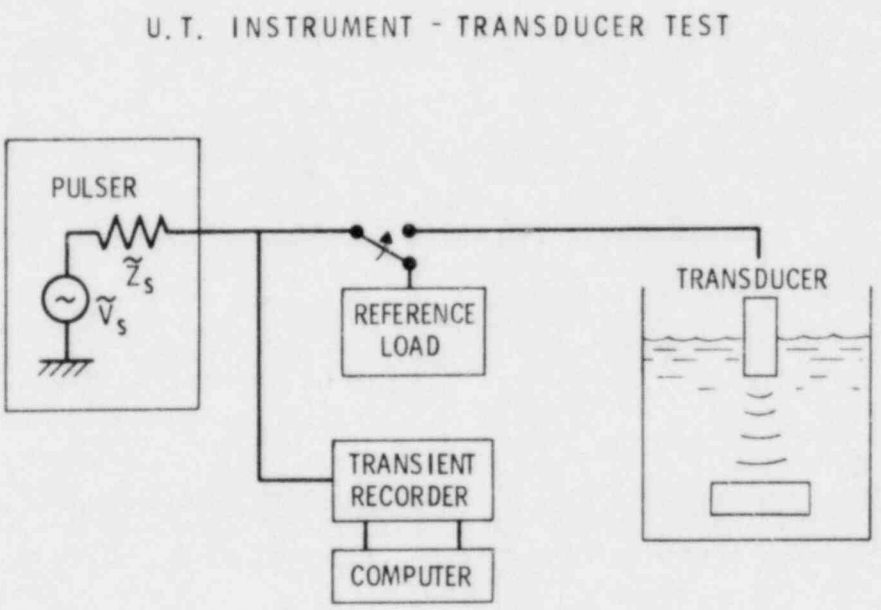

Figure 3. Block Diagram of the System Used for the Evaluation of the Electrical and Electromechanical Properties of a Transducer

For the measurement procedure three different voltage waveforms are recorded experimentally. The first is shown in Figure 4. It is a record of the drive voltage supplied by the pulser into a known and well characterized load--(50 + j0) ohms. The pulse width is determined by the operating frequency of the transducer, and the polarity is chosen to

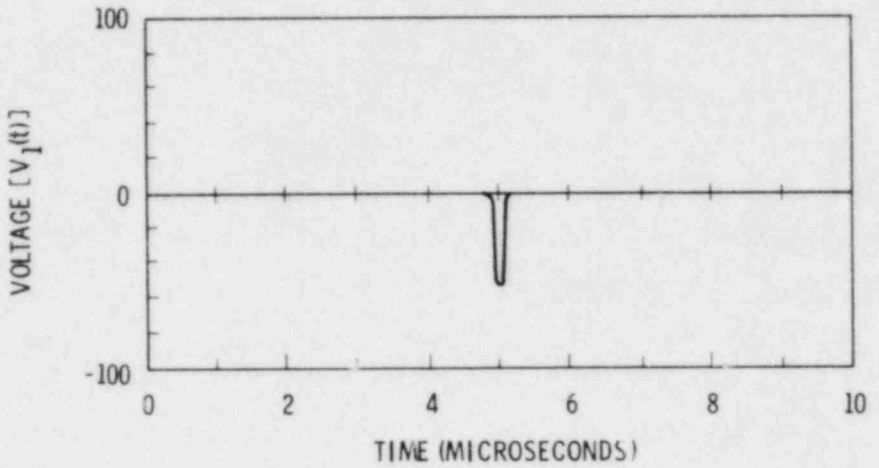

Figure 4. Waveform [$V_1(t)$] Measured with a Reference Load in Place

maintain the convention used in most ultrasonic test equipment. The second waveform recorded is shown in Figure 5. It is obtained by removing the reference load and applying the unknown load; the transducer, loaded by an appropriate mechanical load. For immersion transducers, the appropriate load is water, for contact transducers--metal, and for angled beam

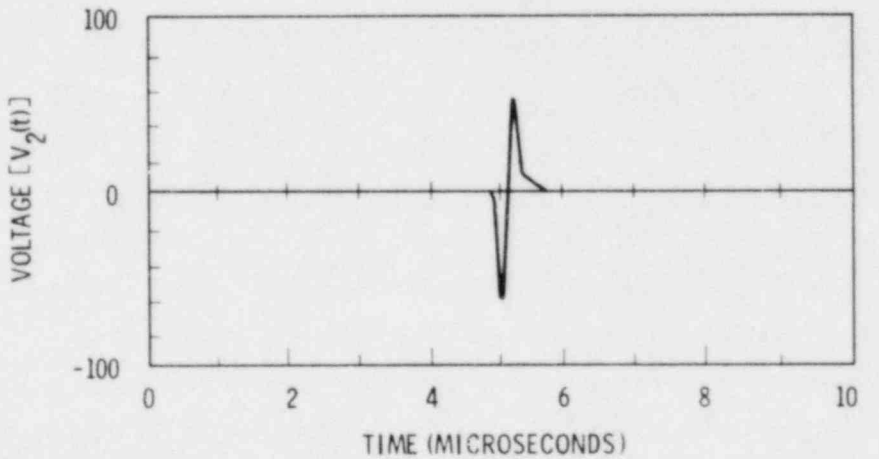

Figure 5. Waveform [$V_2(t)$] Measured with the Unknown Load Presented by the Transducer in Place

transducers--plastic wedge material. Calculation of the complex spectra (real and imaginary parts) and application of Equation (5) allows the complex impedance of the transducer element to be determined. The results of this procedure are shown in Figure 6. This particular transducer was inductively tuned--the reactance is positive below the operating frequency, and the magnitude of the impedance goes to zero at the low frequencies. In the time domain, tuning manifests itself as an inductive overshoot following the turn off of the drive pulse. The power delivered to the transducer is calculated with Equation (6) and is shown in Figure 7.

The third waveform recorded is that of a receive echo obtained from a large specular reflector. For nonfocused, immersion transducers a flat, smooth glass block, not smaller than 3 in. by 3 in. (75 mm by 75 mm) by 1-in. (25-mm) thick is used. This reflector is placed 2 in. (50 mm) from the face of the transducer. (Ideally, the reflector is placed at the near to far field transition (a^2/λ) for the transducer being tested. However, this is impractical for many types of immersion units. Consequently, the lesser distance, either 2 in. (50 mm) or the near-far field transition, is chosen. This compromise appears to work well with a wide variety of transducer diameters and frequencies.) For focused, immersion transducers, a flat glass block located at the focal plane is used as the specular reflector. For normal (straight) beam contact transducers, the back surface echo from a 2-in.- (50-mm-) thick rolled aluminum block is used as the reflector. For angled-beam, contact transducers the corner reflection from a 90^{o} corner in a 2-in.- (100-mm-) thick rolled aluminum block is used as the perfect reflector. Figure 8 shows the results of such a measurement. Panel A) shows the time domain waveform and panel B) shows the relative pulse echo sensitivity. Figure 9 shows the measured and ideal

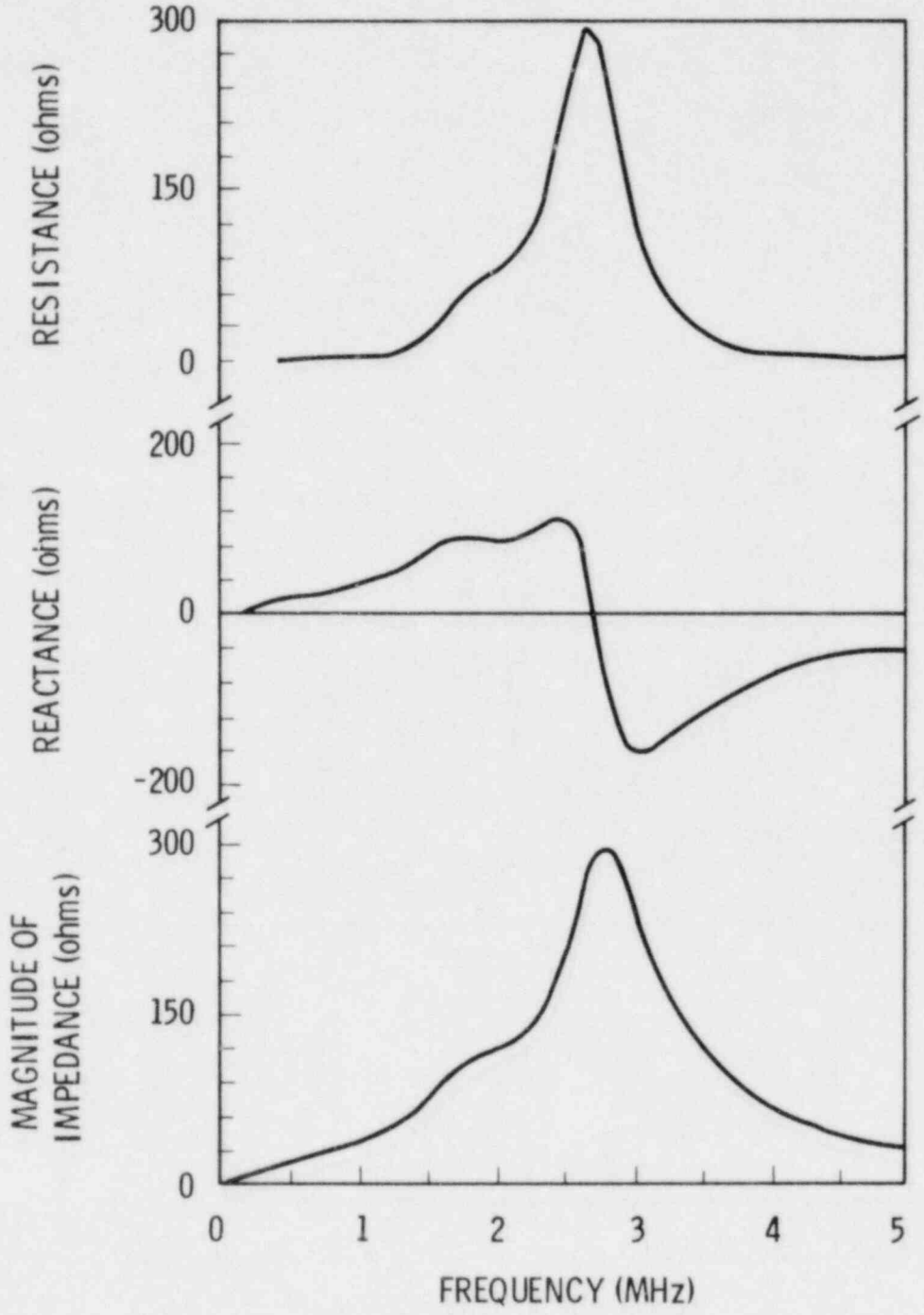

Figure 6. Complex Electrical Impedance of the Transducer Calculated from the Two Observed Waveforms, $V_1(t)$ and $V_2(t)$

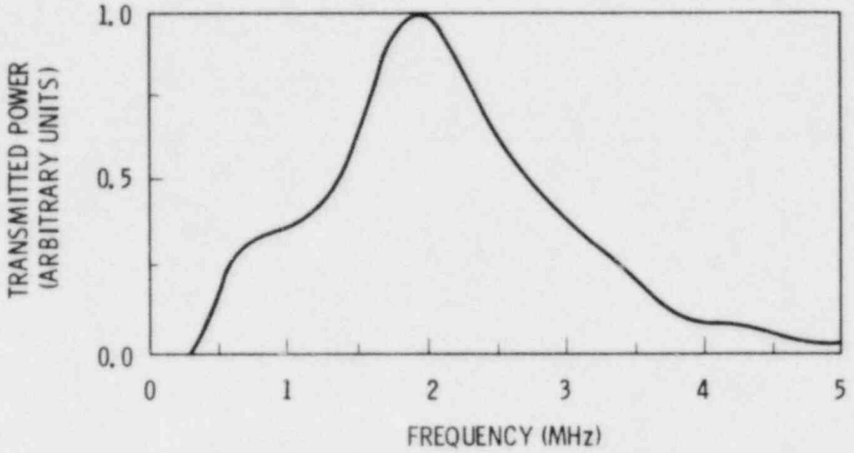

Figure 7. Transmit Power as a Function of Frequency

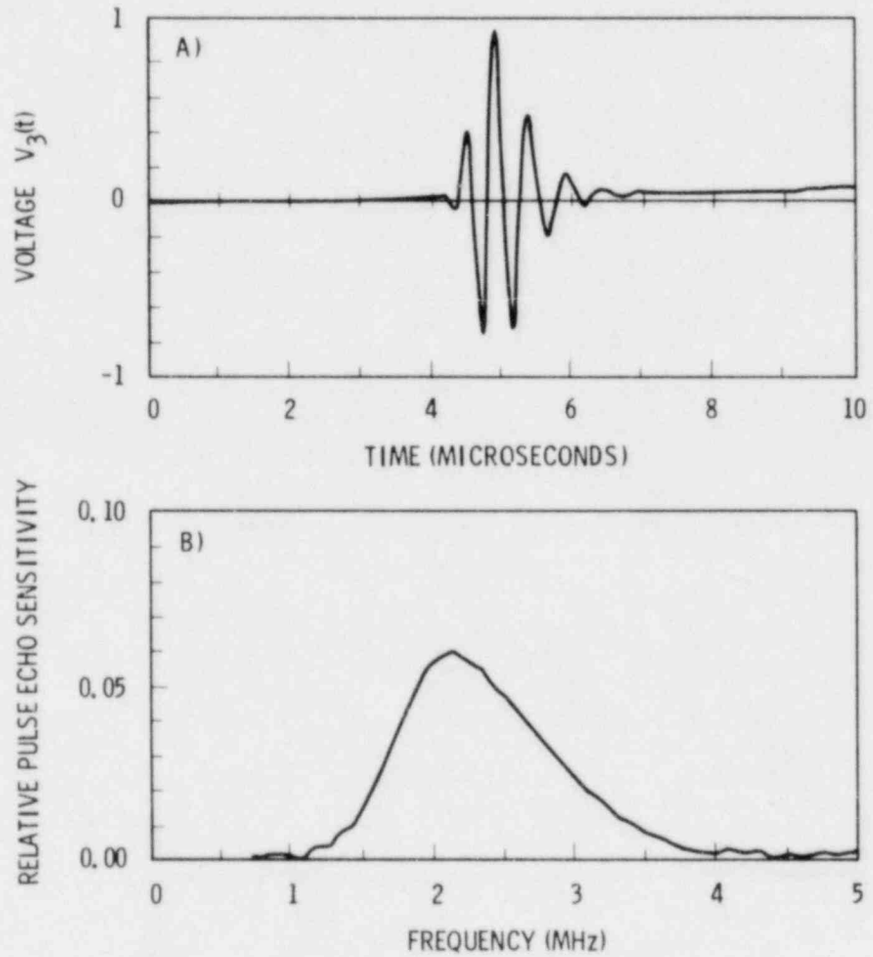

Figure 8. Waveform [$V_3(t)$] Obtained from the Transducer Operating as a Receiver

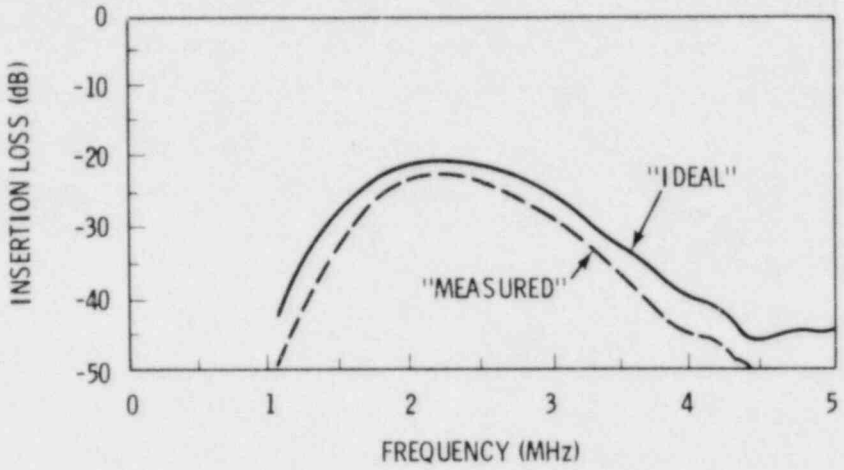

Figure 9. Insertion Loss as a Function of Frequency

insertion loss expressed in decibels after application of the analysis presented in the previous section.

This particular transducer was designed to produce a 45^{o}, vertically polarized shear wave in steel, through the use of a plastic shoe. This unit was characterized with the plastic shoe in place using the corner reflection in the aluminum test block. It is essential to characterize angled-beam transducers with the plastic shoe in place because many transducers of this design employ "matching layers" on the face of the piezoelectric elements which are specifically designed to operate into plastic.

2.3 BEAM PATTERN MAPPING

The mapping of the ultrasonic field pattern produced by a transducer is also important for complete performance evaluation. For immersion transducers, such beam pattern mapping is usually accomplished in a water tank by scanning a point-like receiver or reflector through the ultrasonic beam and recording the transmitted or reflected signal (Papadakis

1977; Posakony 1975). For transducers meant to be used in contact with metal, i.e., contact or angled-beam transducers, beam mapping procedures have been developed using point-like reflectors within the metal test block and also using small, noncontacting electromagnetic transducers (EMATs) to map the ultrasonic field within the metal part (Wuetenberg 1970, 1979).

The scanning EMAT technique has been implemented at PNL to map the sound field produced in metal by 45-degree and 60-degree, shear wave transducers. Figure 10 shows schematically the test block now in use. The block is made of A533 steel and has been machined to have a flat top surface with angled sides. The angled side surfaces were machined at

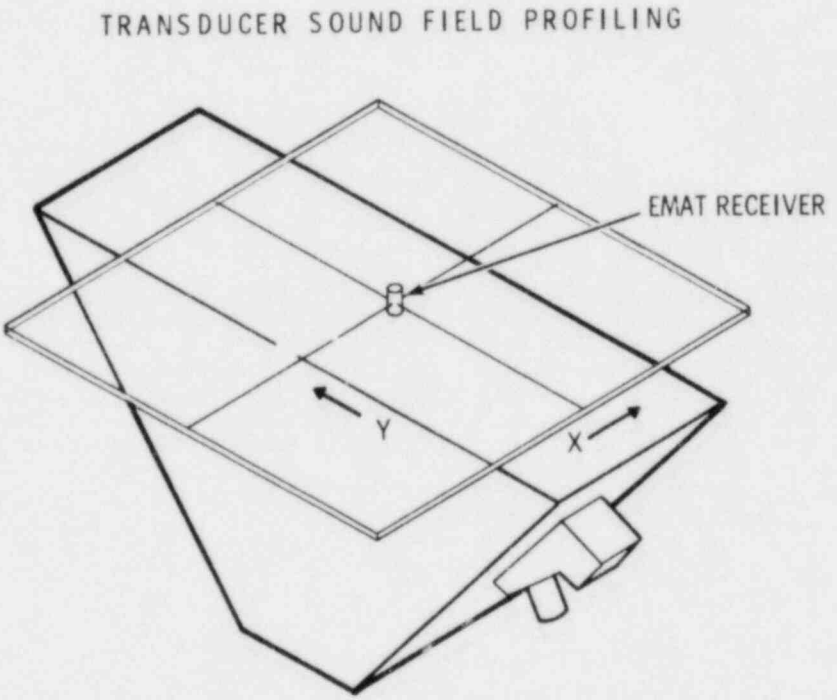

Figure 10. Calibration Block Used to Map the Sound Field Produced by Angled Beam Transducers in Metals

angles of 30^{o} and 45^{o}, respectively, with respect to vertical. These angles were chosen so that 60^{o} and 45^{o} shear wave transducers would produce a sound field that would be incident at right angles upon the upper surface of the block. By scanning the EMAT in a "raster" fashion over the top surface, a two-dimensional profile of the transducer sound field pattern is obtained. This procedure can be repeated for a number of different metal paths to more completely characterize the beam spreading or focusing properties of the transducer under test.

Figure 11 shows a block diagram of the electronics associated with this system. The ultrasonic and the scanner

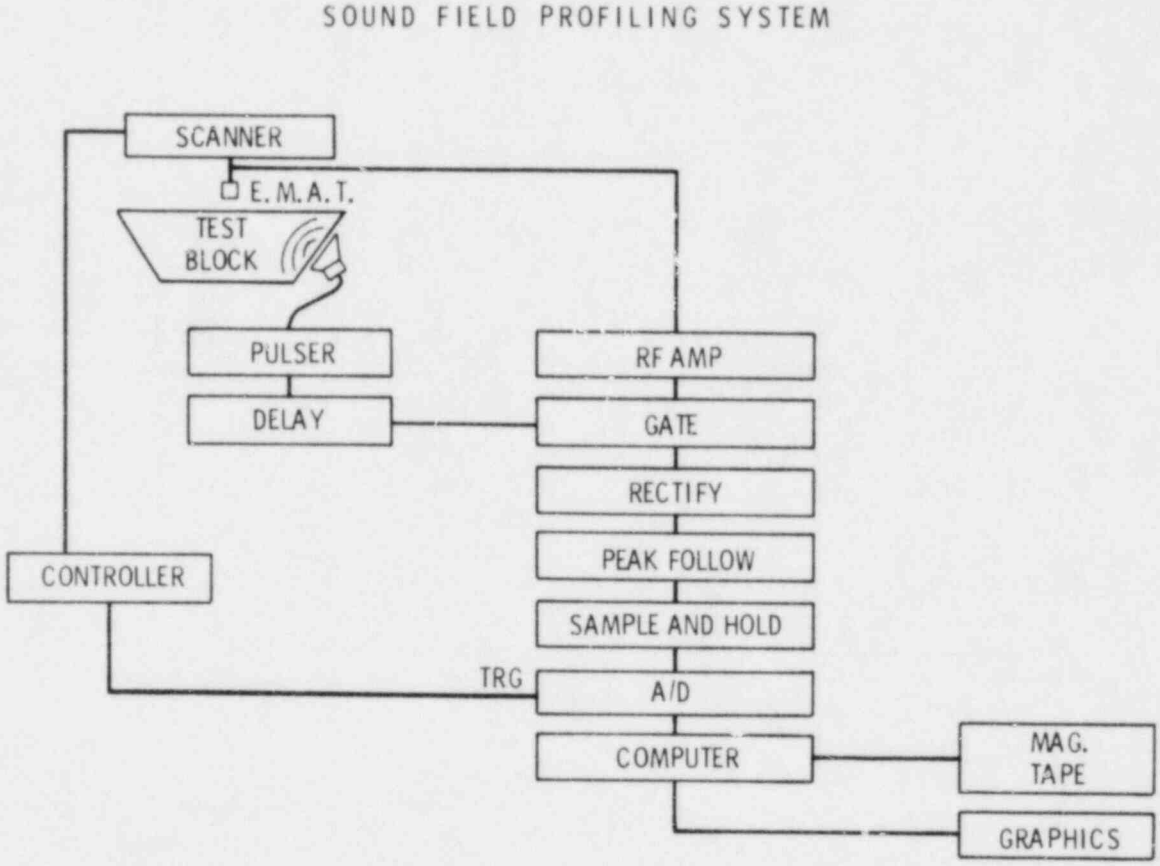

Figure 11. Block Diagram of the Electronics of the Sound Field Profiling System

systems are basically separate systems which run independently and are simultaneously monitored by the computer. The output of the ultrasonic system is a DC voltage which represents the amplitude of the ultrasonic pulse sensed by the EMAT probe. The output of the scanner system is a train of pulses which are derived from the pulses used to drive the stepper motors of the scanner. These pulses act to trigger the analog-to-digital converter. This scheme for data collection works well as long as the ultrasonic repetition rate is greater than the rate at which trigger pulses are sent to the A/D converter. At present, measurements are made over a 2-in. by 2-in. (50-mm by 50-mm) aperture with one measurement every 0.024 in. (0.6 mm). This results in the generation of nearly 6900 data points for each beam profile. This data is recorded on magnetic tape for permanent record and subsequent re-display. Figure 12 is an example of this beam profile

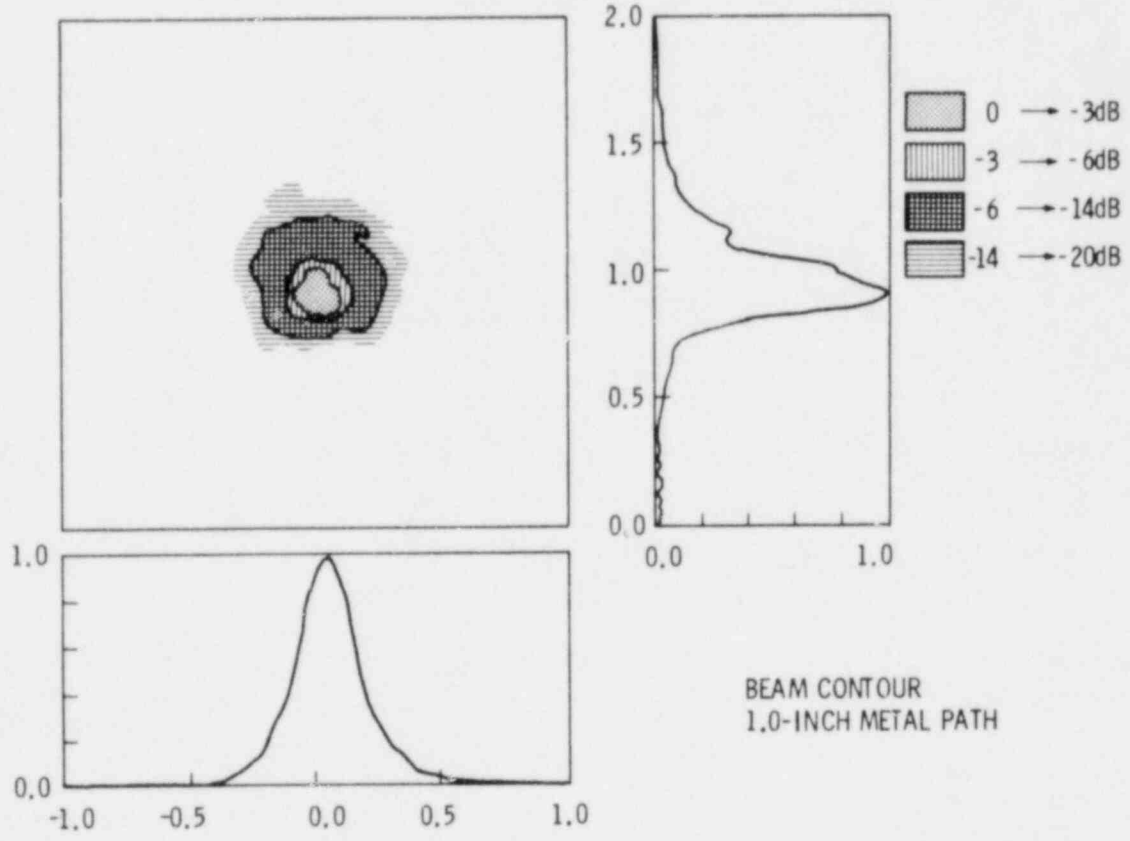

Figure 12. Example of the Output of the Sound Field Profiling System

data. A contour map is produced as well as two linear "scan line" plots through the maximum of the contour map. The original presentation of the beam profile data is done in color with contour levels chosen as follows: 0 to -3 dB, -3 to -6 dB, -6 to -14 dB, and -14 to -20 dB. Other contour levels can be chosen when the data is re-displayed. The x scan direction corresponds to lines of constant metal path within the test block and the y scan direction corresponds to lines with variable metal path (see Figure 10 for detail).

Figure 13 presents the results of measurements made using two different 2.25-MHz transducers with a 1-in. metal path distance. Panel A of the figure shows the beam produced by a 1/2-in. by 1/2-in. (12.5-mm by 12.5-mm) square transducer, and panel B shows the beam produced by a 1/2-in. (12.5-mm) circular transducer. Figure 14 shows data taken from these same transducers when the metal path is increased to 3.0 inches.

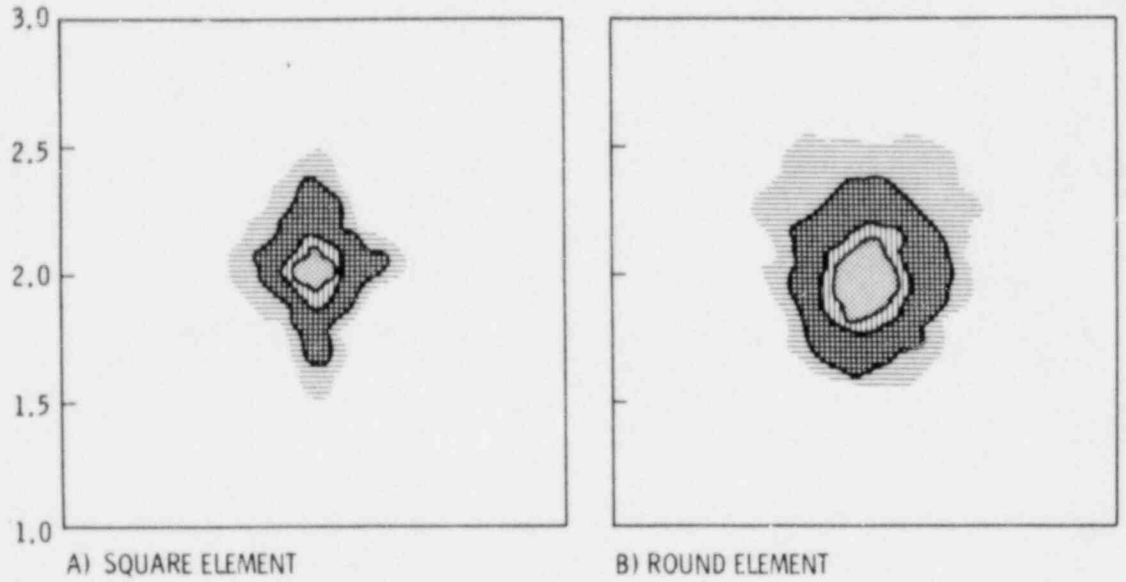

Figure 13. Comparison of Beam Profiles Produced by Different-Shaped Transducers.

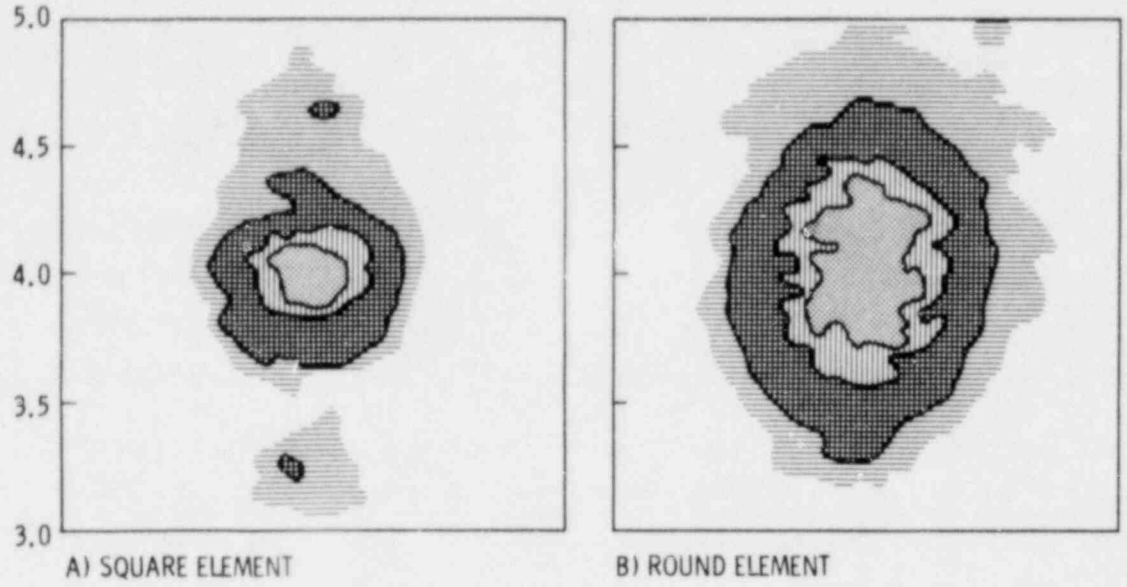

Figure 14. Comparison of Beam Profiles Produced by Different-Shaped Transducers

PNL has formulated a procedure for the evaluation of dual-element search units. Since the overall transducer response of a dual-element transducer depends upon the combined beam patterns of the transmitting and receiving element, this evaluation procedure must measure both beam patterns independently and then combine them in an appropriate fashion.

The relative spatial pulse echo response (p^{PE}) of the dual-element search unit can be estimated by multiplication of the independently measured beam patterns, p^1 and p^2:

$$|p^{PE}(x,y)| = |p^1(x,y)| \times |p^2(x,y)|. \qquad (16)$$

Because only the magnitudes of the field patterns are measured, $|p^1|$ and $|p^2|$, no interference effects are produced by forming this product. This seems to be a fair representation of the combined beam pattern because the physical "fields" from the two different transducers are not simultaneously present and therefore cannot interfere with one another.

This method of combining the two beams allows the spatial response of the transducer to be estimated as if the transducer had been scanned past a point-like reflector in the metal. Figure 15 shows this pulse echo beam pattern near the overlap region of the two beams, P^1 and P^2, and Figure 16 shows the beam pattern for a metal path of 3.0 inches. The three plots shown in the horizontal scan lines are 1) individual profile from the right element (dotted line), 2) individual profile from the left element (dashed line), and 3) multiplied profile (solid line). The curves have been normalized with respect to the multiplied profile. The 3-dB beam width of the dual-element transducer is seen to increase somewhat when the metal path distance is doubled;

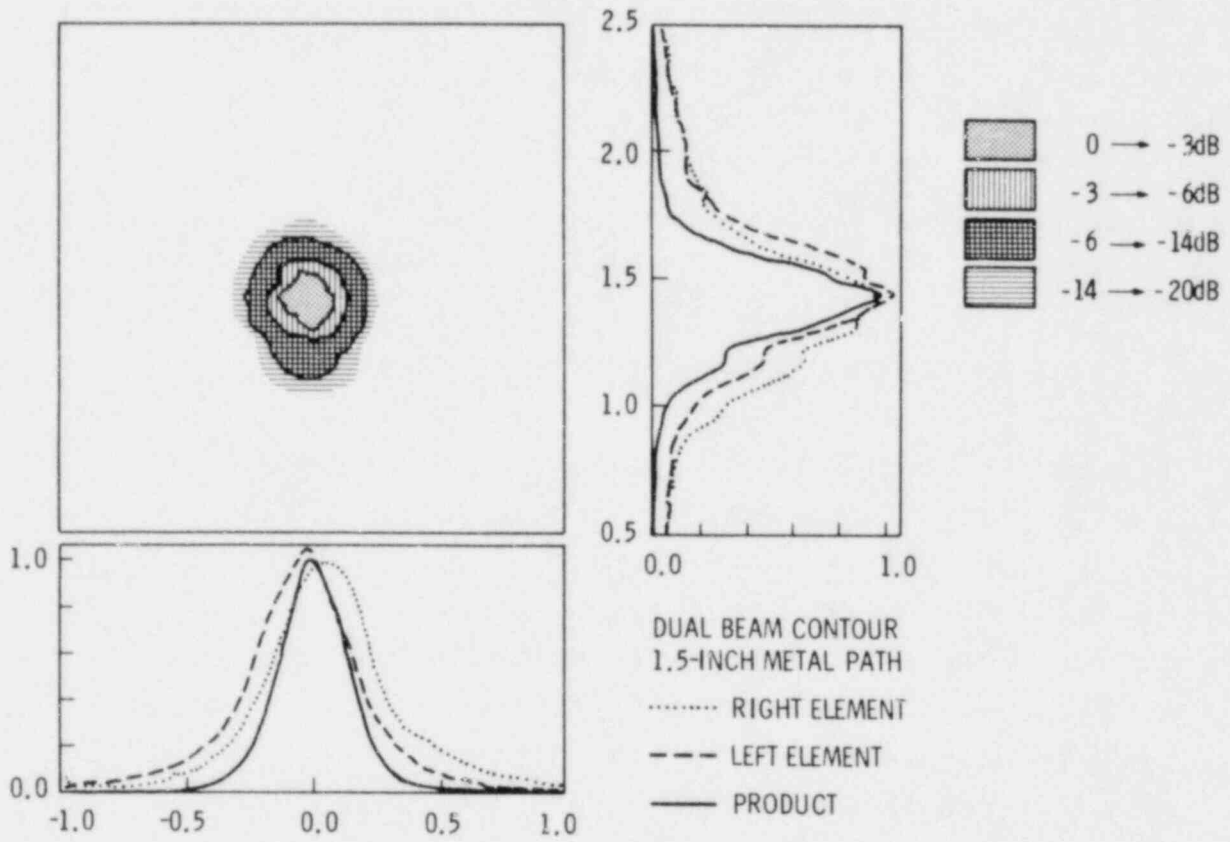

Figure 15. Sound Beam Profile Produced by a Dual-Element, Angled Beam Transducer (metal path length: 1.5 in.; operating frequency: 1.5 MHz)

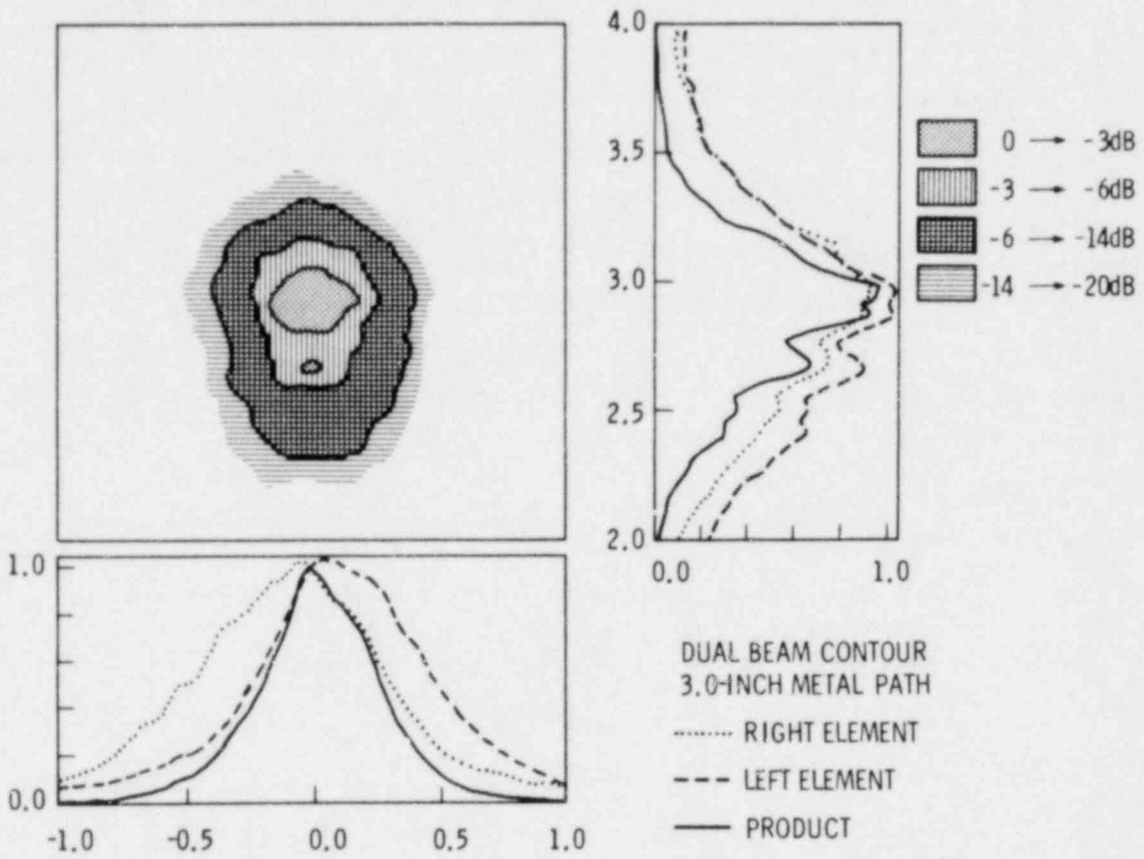

Figure 16. Sound Field Produced by a Dual-Element, Angled Beam Transducer (metal path length: 3 in.; operating frequency: 1.5 MHz)

however it does not broaden as much as the beam patterns from the individual elements. This behavior is similar to the focusing properties observed with an axicon transducer (Burckhardt, Hoffman and Granchamp 1973). In general, the multiplied beam that represents the two-way response of the transducer appears sharper (i.e., more spatially compact) than the single element sound field patterns. The multiplied beam pattern is useful for understanding the observed pulse echo response of these dual-element search units.

3.0 RECEIVER-DISPLAY CHARACTERIZATION

The receiver-display portion of an ultrasonic test instrument is the second major component characterized. The receiver is treated as a "Black Box" with an RF input port and the scope screen or chart recorder output at the output port. This approach to receiver characterization allows only total performance from a functional point of view to be evaluated. If a problem is indicated, a more detailed evaluation would be necessary to isolate the problem to a particular signal processing stage (e.g., detector, rf filter, video amplifier, etc.) within the instrument.

The overall measured properties of the receiver-display subsystem include receiver bandwidth, linearity, noise level referred to the input, and sensitivity referred to the input. As described by the test results, these properties can vary as the RF gain, video gain, RF filtering, and video filtering of the instrument are changed.

3.1 MEASUREMENT SYSTEM

A semi-automated measurement system has been assembled by PNL to facilitate the characterization of ultrasonic test equipment. A block diagram of this system is shown in Figure 17.

The output pulse from the pulser section of the instrument being tested provides the "clock" pulses for this system. The limiter circuit/pulser combination provides a pulse of fixed duration to the programmable oscillator. This pulse is used to "gate" the oscillator. A burst of RF, approximately 10 microseconds long, is the input to the receiver section of the instrument under test. The time delay between transmitter output and receiver input pulse is controlled by the computer, as is the amplitude and frequency of the oscillator. By simultaneously varying the time delay and the

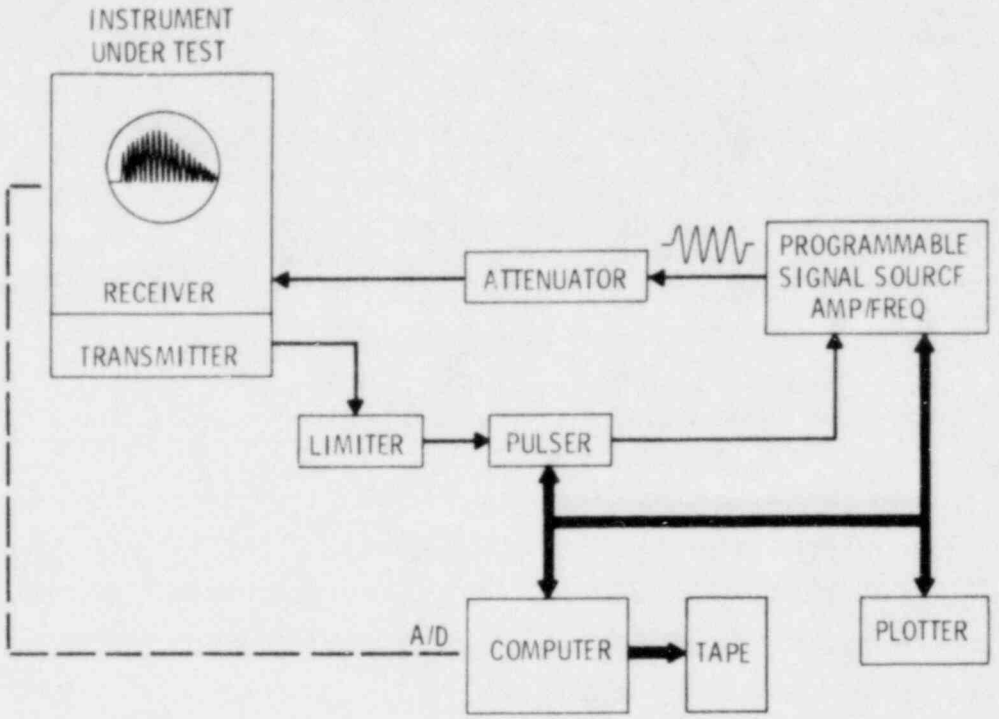

Figure 17. Block Diagram of the Electronics Used to Characterize the Performance of the Receiver-Display

oscillator frequency, a plot of the frequency response of the tested instrument is displayed on the instrument's scope screen. The linearity of the instrument can be evaluated in a similar manner.

For instruments that provide no analog signal output, the operator plays a critical role in the instrument evaluation. He is required to manually make measurements from the instrument scope screen and key them into the computer. For instruments that provide an analog output, the A/D converter can be used to totally automate the data collection process.

3.2 INPUT NOISE AND INPUT SENSITIVITY MEASUREMENTS

The measurement of the input noise and sensitivity are accomplished by the operator. The input noise recorded refers to the amount of noise in microvolts RMS referred to the input when the input is terminated into 50 ohms. This measurement is generally made with the instrument at full gain. The input noise is estimated using a simple measurement technique which requires only an oscilloscope (Franlin and Hatley 1973; Gruchaila 1980). If the input noise is too high to make this measurement at full gain, the gain is reduced to a point where the noise can be measured. The quoted value of input noise is normalized as if it had been measured at full gain.

The input sensitivity of the receiver is defined as the amount of signal in microvolts RMS required at the input of the receiver, when the input is terminated into 50 ohms, to deflect the CRT trace to 50% of full scale. This measurement is either made with the instrument operating at full gain or else normalized to the full-gain condition.

3.3 MEASUREMENT RESULTS

In this section a series of measurements made upon the receiver-display sections of two commercially available ultrasonic test instruments are presented. The purpose of presenting these results is twofold: 1) to demonstrate how the response of a single instrument is affected by changing RF filtering and the video filtering of the instrument, and 2) to demonstrate the variation between different instruments observed when nominally similar setup procedures have been followed. Results are presented in terms of instrument frequency response and linearity. The results are intentionally presented in a manner that preserves the anonymity of the instrument manufacturer.

3.3.1 Frequency Response Measurements

In Figure 18, the frequency response as measured from a commercially available instrument, Model 1, are shown. The observed output (screen deflection) is plotted as a function of the frequency of the input tone burst for a fixed input amplitude. The three curves plotted in Figure 18 refer to three different positions of the RF filter setting of the instrument; 1.0, 2.25, and 5.0 MHz. The RF filter setting appears to have two effects upon the instrument performance: 1) the setting determines the frequency of the peak of receiver response and 2) the setting changes the overall sensitivity of the instrument. In Figure 19, the performance of Model 1 for different filter settings (5.0, 10.0, and wide band) is shown over a somewhat broader (0 to 20 MHz) frequency range. Examination of Figures 18 and 19 indicate a good correlation between the peak frequency of operation and the indicated filter position for all settings except wideband. The wideband position exhibits a peak response at approximately 2 MHz. The 10 MHz filter position appears to provide a broader frequency response than the wideband position. It should also be noted that for Model 1, the instrument sensitivity is strongly affected by the RF filter position. Several instruments of this model were evaluated. The results obtained are consistent on a unit to unit basis.

Figure 20 shows the results obtained from measurements made upon a second commercially available ultrasonic test instrument, Model 2. Measurements were made with the RF filter of the instrument set at 1.0, 2.0, and 5.0 MHz. The sensitivity of Model 2 does not appear to be strongly affected by RF filter position. The frequency of maximum response, however, does not appear to be well correlated with RF filter position. Figure 21 shows the response of Model 2 over a broader frequency range at two different RF filter positions;

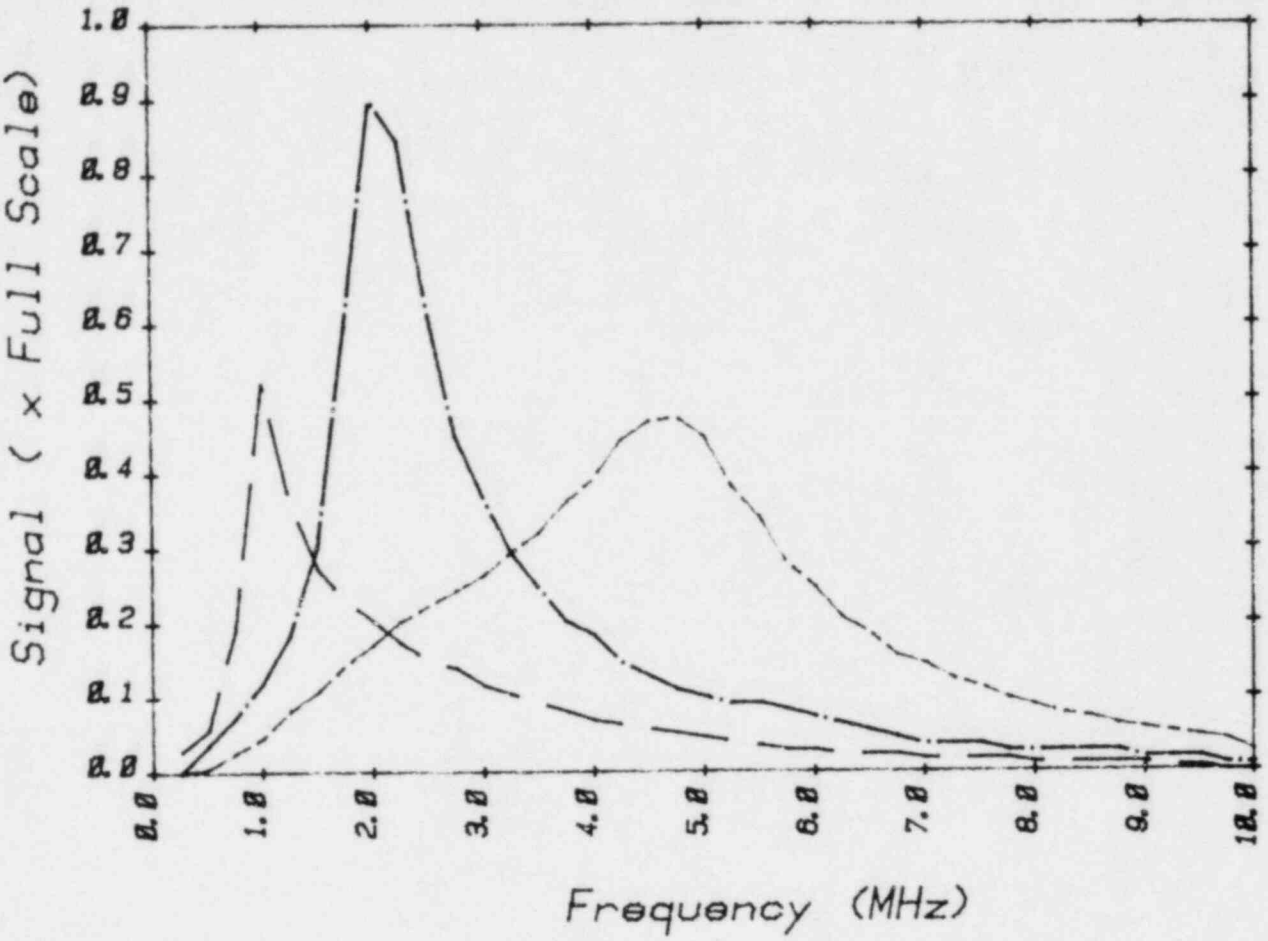

	INPUT NOISE (uVolts)	SENSITIVITY (uVolts)
— — — 1.0 MHz	5.0	62.8
—·—·— 2.25 MHz	3.5	35.6
- - - - - 5.0 MHz	4.5	62.9

Figure 18. Frequency Response of the Receiver-Display Portion of a Commercially Available UT Instrument (Model 1)

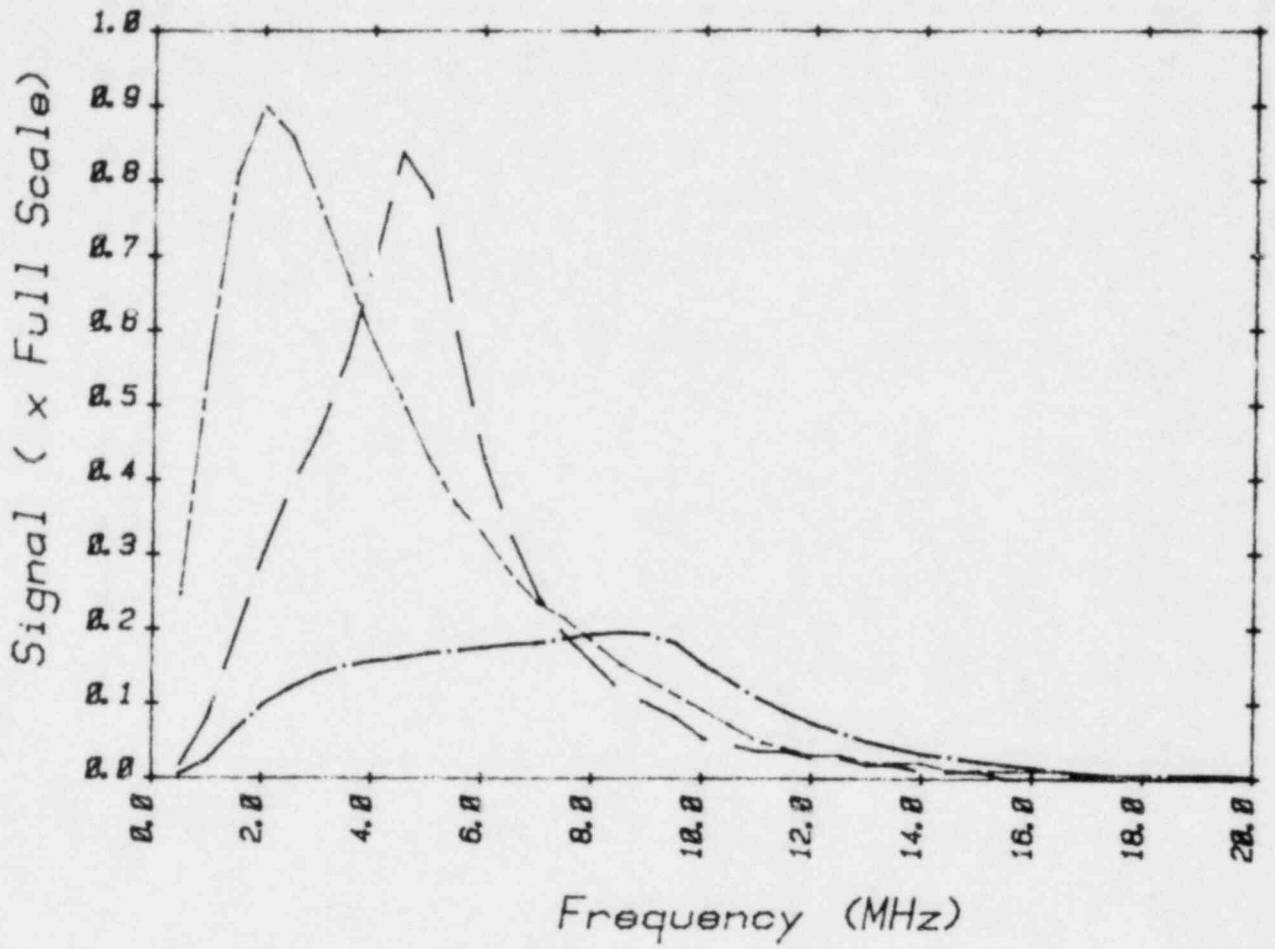

	INPUT NOISE (uVolts)	SENSITIVITY (uVolts)
5.0 MHz	4.5	62.9
10.0 MHz	11.2	250.3
WB	4.5	62.9

Figure 19. Frequency Response of Model 1 over a Broader Range of Frequencies

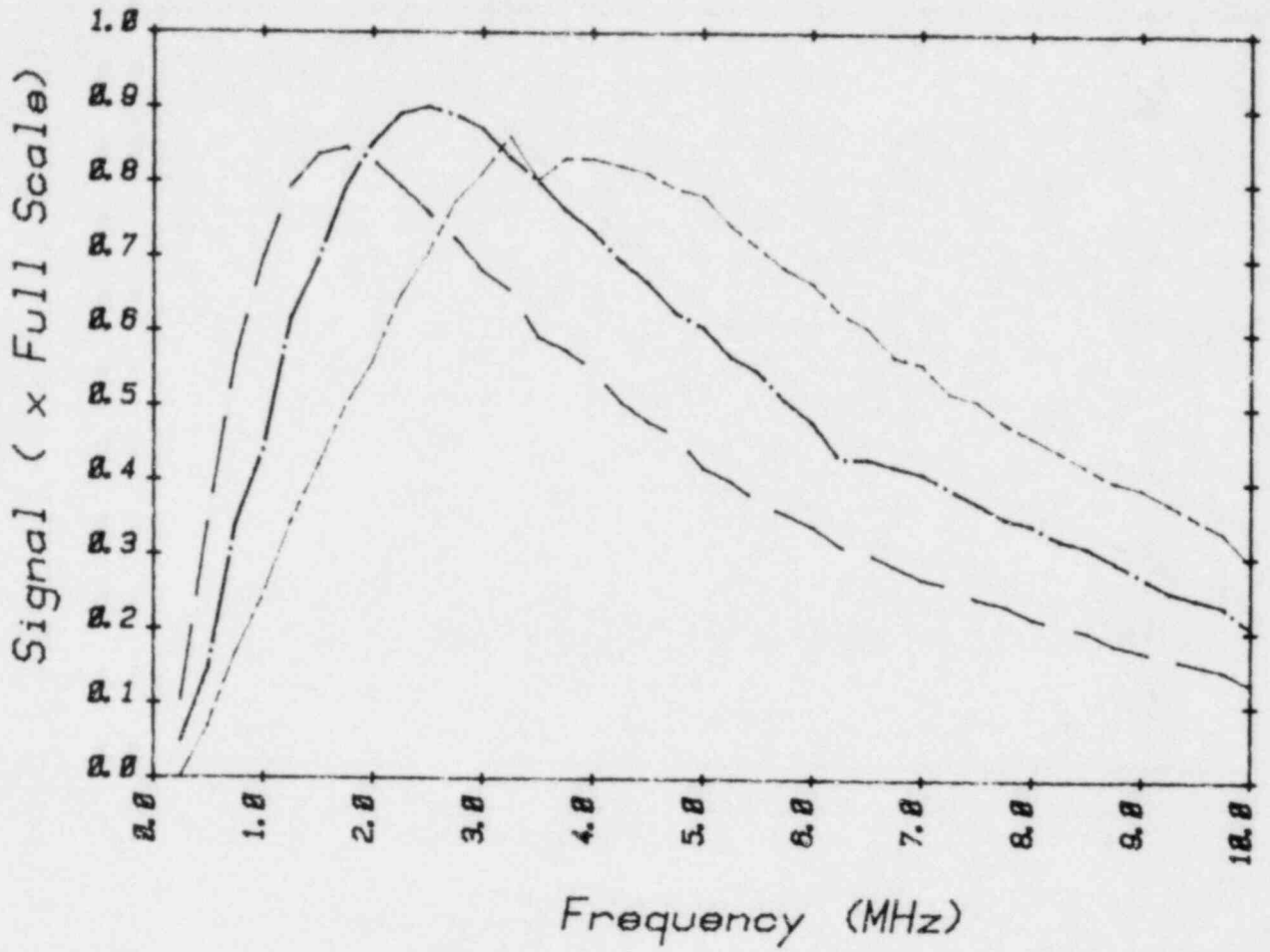

	INPUT NOISE (uVolts)	SENSITIVITY (uVolts)
1 MHz	11.2	62.9
2 MHz	11.2	62.9
5 MHz	11.2	70.5

Figure 20. Frequency Response of a Second Commercially Available UT Instrument (Model 2)

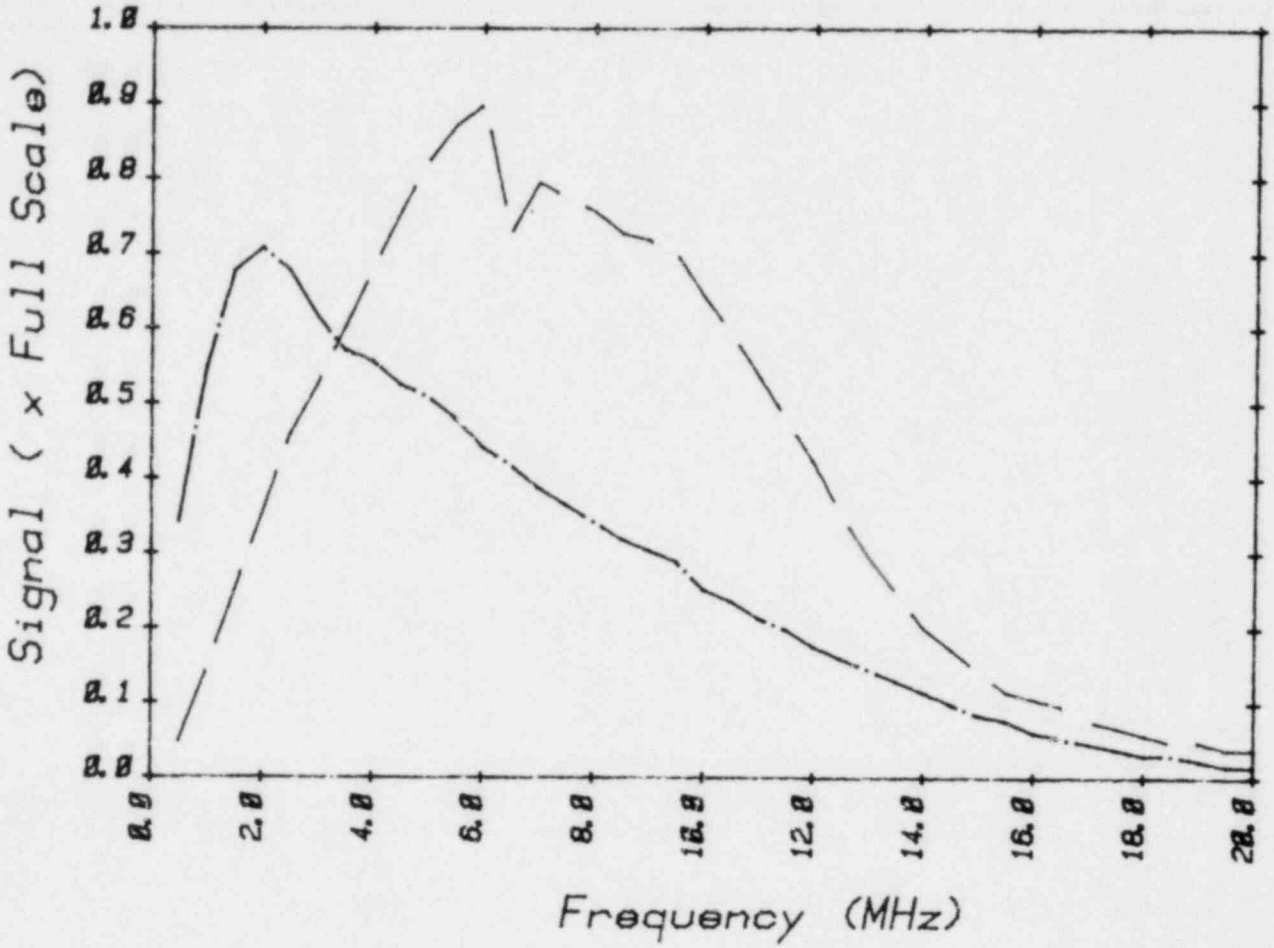

	INPUT NOISE (uVolts)	SENSITIVITY (uVolts)
— — — 10 MHz	15.8	44.5
—·—·— B	11.2	56.0

Figure 21. Frequency Response of Model 2 over a Broader Range

10 MHz and broadband. The discontinuity in the response of Model 2 on the 10-MHz filter position is noticeable and is a reproducible feature of this instrument's performance. As noted with Model 1, the 10-MHz filter position of Model 2 appears to provide a broader frequency response than the broadband position. Again several instruments of this model were evaluated to insure the test results were not unique to a single instrument.

3.3.2 Linearity Measurements

Figure 22 presents the linearity as measured from Model 1. The observed output is plotted as a function of RF input amplitude for a fixed tone burst center frequency of 2.25 MHz. The three curves plotted in Figure 22 refer to three different positions of the video filter in the receiver of the instrument. The receiver is linear for two of the three video filter positions, however, the third filter position produces a limited or compressed output. Similar results for Model 2 are presented in Figure 23. Measurements for Model 2 were made at 2.0 MHz. The output amplitude of Model 2 is seen to be linearly related to the input amplitude for all video filter positions tested. The system gain (slope of curve) appears to be affected somewhat by the video filter position.

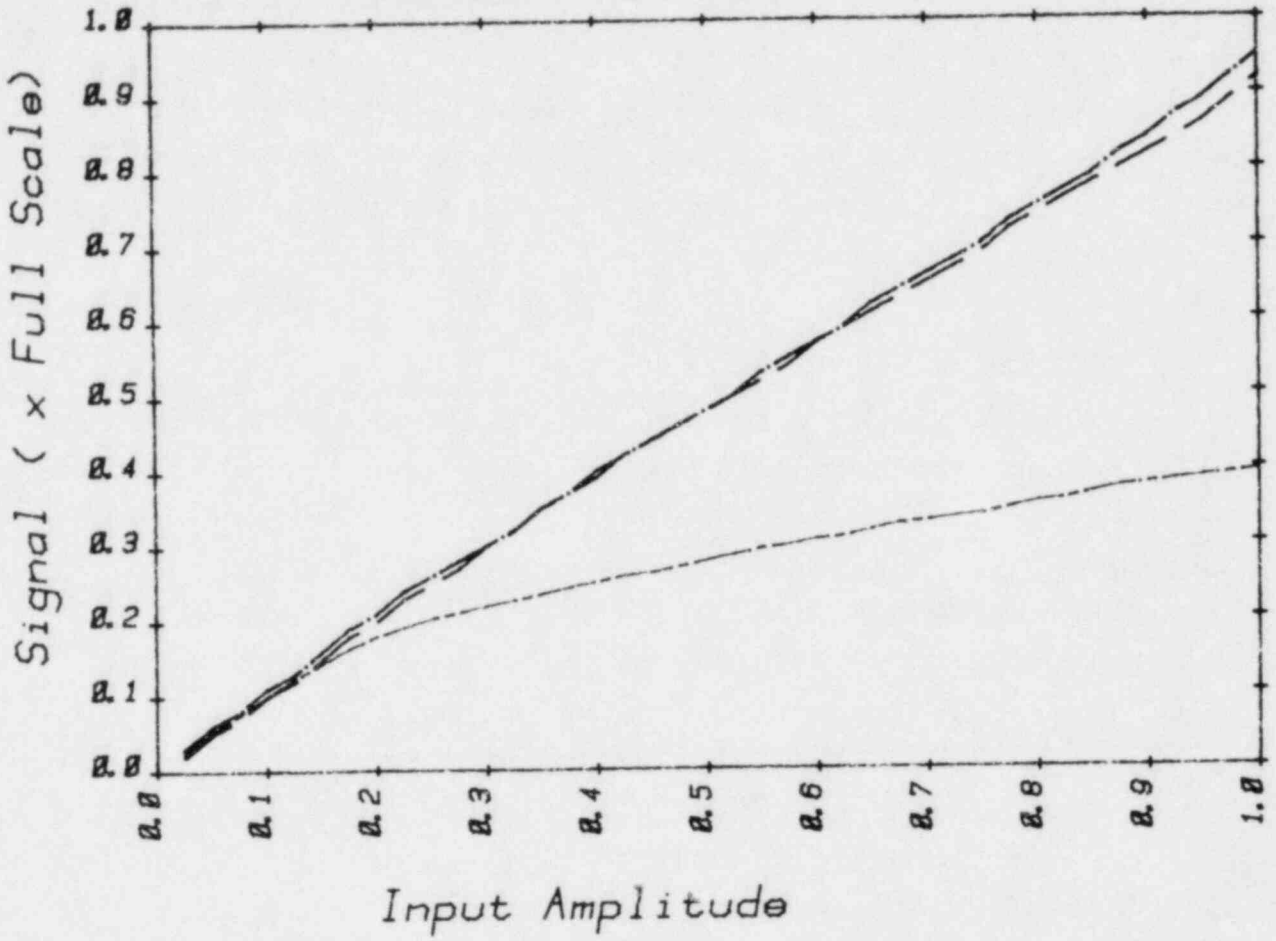

Figure 22. Results of Linearity Test Upon Model 1

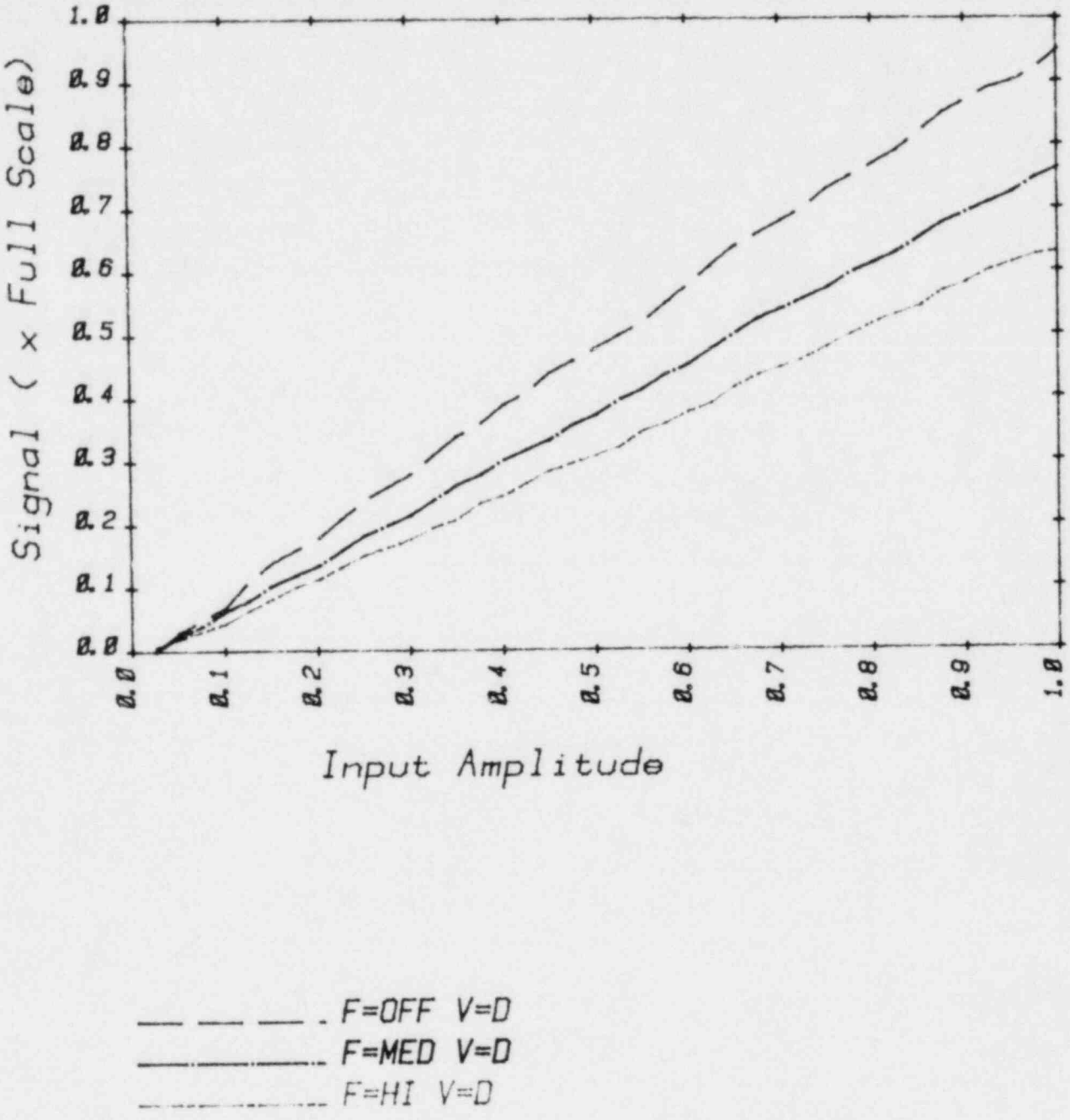

Figure 23. Results of Linearity Test Upon Model 2

4.0 PULSER CHARACTERIZATION

By far the most difficult portion of the ultrasonic test system to characterize fully is the pulser or transmitter subsystem. This difficulty arises because of the inherent nonlinearity built into these circuits. Avalanche diodes and silicon control rectifiers are commonly used by manufacturers, and these components are difficult to characterize using simple linear circuit theory. Proper characterization of these circuits requires a more general circuit theory that is able to handle modest nonlinearities. Such an approach would model the transmitter output "impedance" as a Volterra Series and would allow the resistance and reactance of the circuit as well as higher order impedance terms to be determined (Volterra 1959). This approach, while correct in theory, was not implemented because the utility of the nonlinear impedance information was not clear.

The procedure used by PNL to describe pulser performance was to record the time domain voltage waveform produced across two different, known electrical loads. From these measurements the power spectral content of the drive pulses can be derived as well as a Thevenin equivalent circuit for the pulser. The equivalent circuit provides useful information about the effective output impedance of the pulser. This estimate of output impedance allows the efficiency of the pulser to be estimated for a wide variety of transducer loads.

Figure 24 shows a block diagram of the present measurement system. The sampling scope is used rather than a transient recorder because it can be used to record much faster events. The two electrical loads are 50 ohms (from a standard terminator) and 500 ohms (the input impedance of the high-voltage probe). Typical time domain signals are shown in Figure 25A. The power spectra of the transmitted pulse

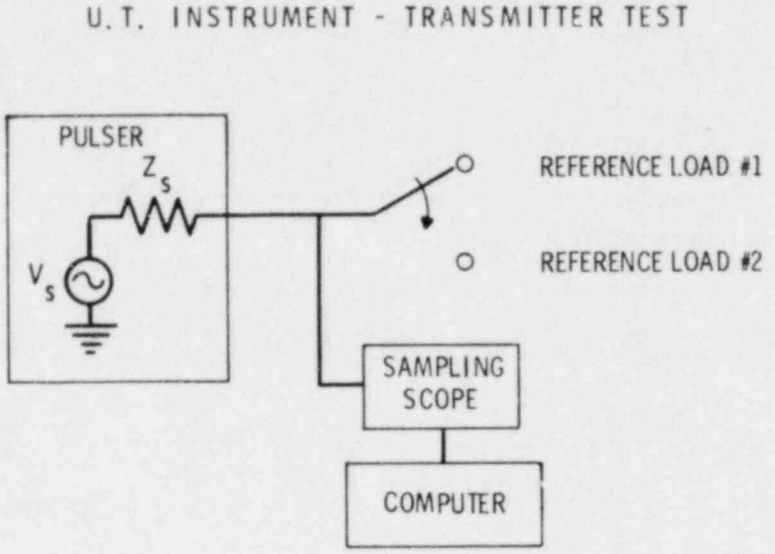

Figure 24. Block Diagram of the System Used to Characterize the Transmitter of Pulser

into these two reference loads is shown in Figure 25B. In these plots the 0 dB refers to a 100-volt continuous wave input. In other words, the electrical energy delivered by the 300-volt transient electrical pulse into 50 ohms at 5 MHz is equivalent to the energy delivered by a 5-MHz oscillator running continuously at an amplitude of approximately 15 volts (-16 dB relative to 100 volts). From the observed power spectra, as the electrical load which the pulser is required to drive is decreased the high-frequency content of the electrical drive pulse is not diminished as much as the low-frequency content of the pulse. Both of the curves in Figure 25 were taken with the internal damping control at its minimum setting.

Figure 26 shows the effect of using a maximum value of the internal damping adjustment (some instruments refer to this setting as the minimum pulse length). In this case, the

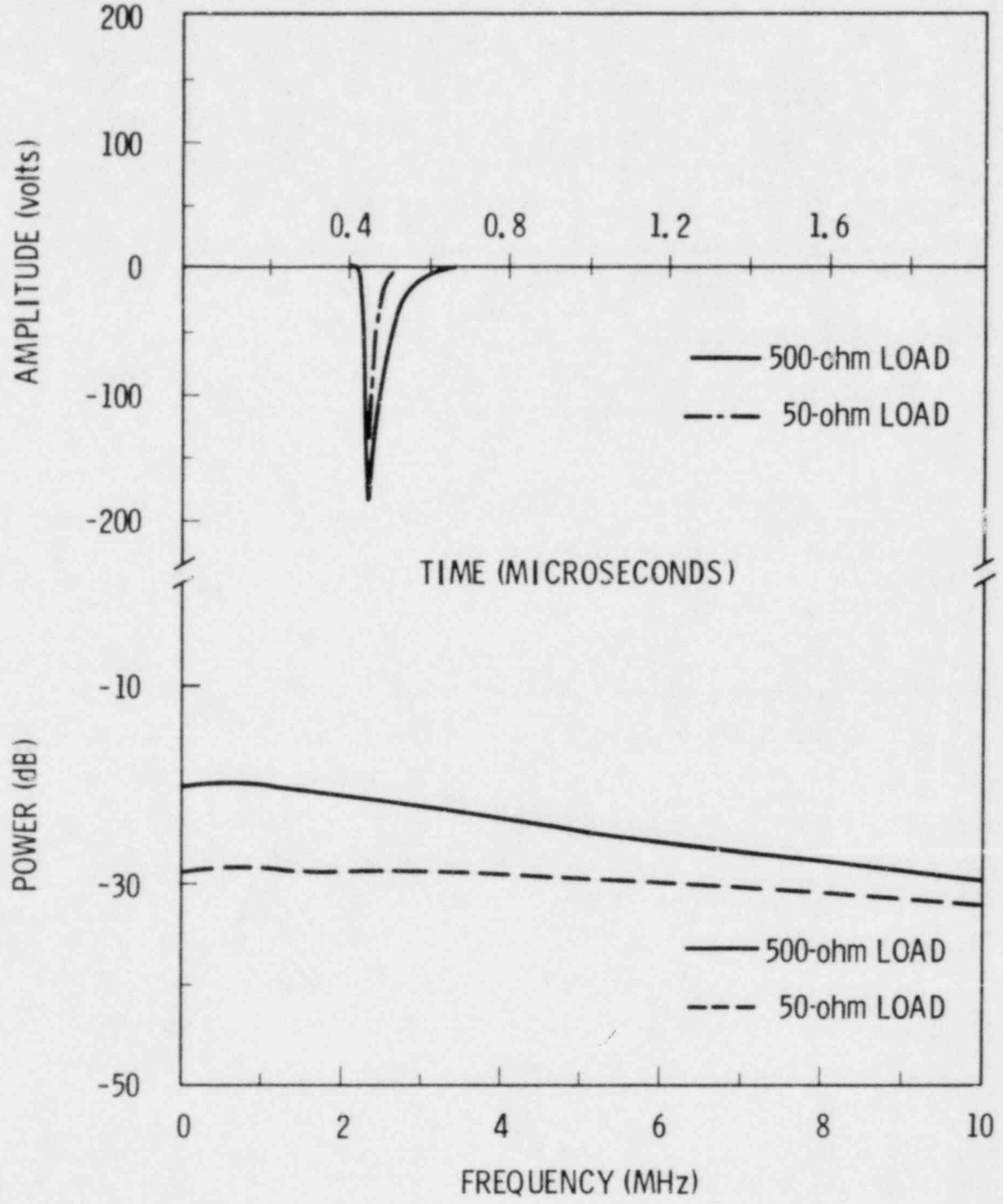

Figure 25. Results of Measurements Made Upon the Pulser Subsystem of Model 1

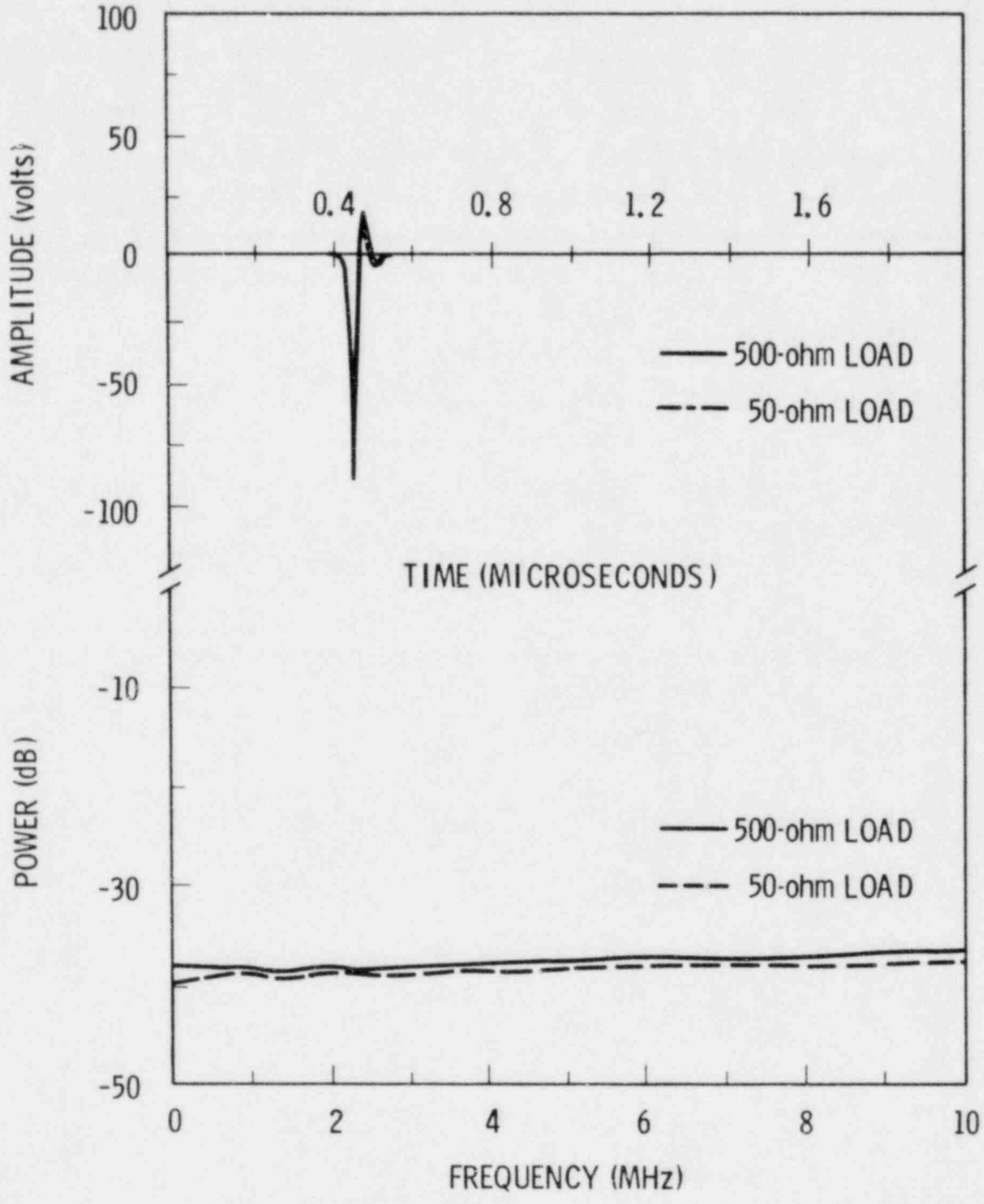

Figure 26. Measurements Made Upon Pulser Subsystem of Model 1 with Maximum Damping

effect of the external load is minimal. Most of the electrical pulse has been "shorted out" internally in the instrument. As a result, a decrease in transmitter efficiency of 15 dB at 2.25 MHz into a 50-ohm resistive load is noted.

An estimate of the magnitude of the output impedance of the pulser can be made using linear circuit theory. The equivalent circuit assumed is similar to that shown in Figure 1; however $\tilde{Z}_\ell$ is replaced by a second reference load of (500 + j0) ohms. Under these conditions, the output impedance of the pulser can be calculated as:

$$Z_S = 500(V_2 - V_1)/(10V_1 - V_2) \qquad (17)$$

Because of the limitations of linear circuit theory, only the magnitude of Z_S is displayed in Figure 27. The output impedance is seen to be quite low and uniform when the

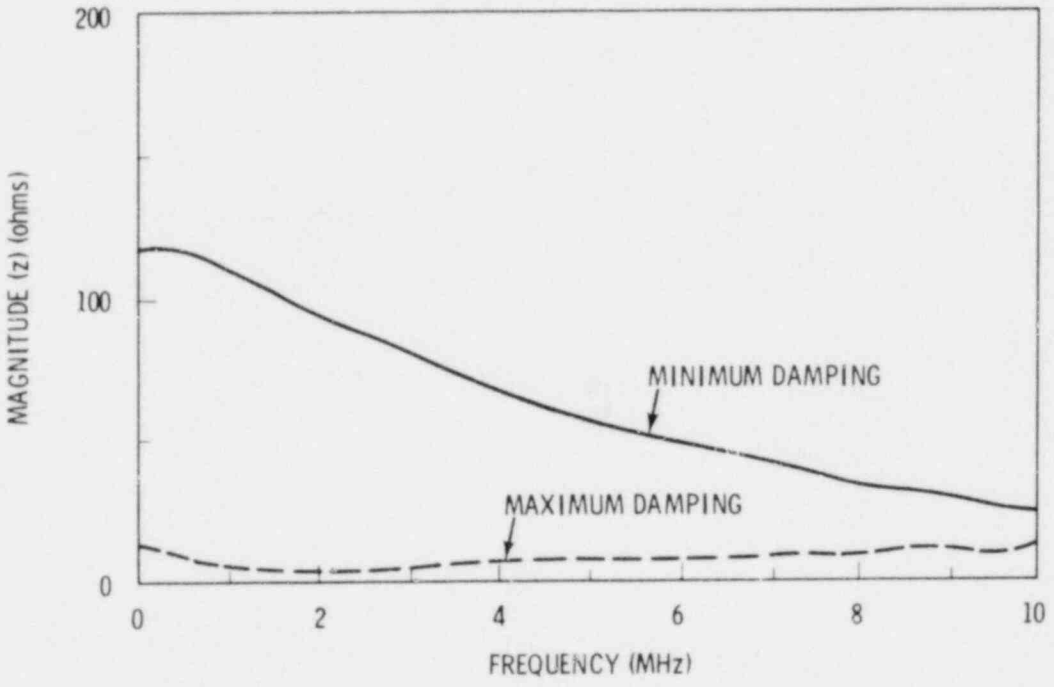

Figure 27. Calculated Output (Source) Impedance of the Pulser Subsystem of Model 1 for Two Different Damping Settings

instrument is used with a maximum value of the internal damping adjustment. With minimum damping, the output impedance rises sharply at lower frequencies, indicating the capacitive nature of this pulser circuit.

This type of analysis (based upon linear circuit theory) although not entirely proper, has been found to be of value for estimating output impedance and for making comparison of different pulser units.

5.0 DISCUSSION

A series of measurement techniques have been presented which are being used to quantify the overall performance characteristics of ultrasonic test instruments. The instrument was considered as three subsystems--a transducer or search unit, a receiver-display, and a pulser. The methods presented were chosen because they provide information about instrument performance. In addition, these methods lend themselves to automated or computerized data gathering and analysis techniques. Simplified evaluation techniques for use in the field are under investigation and will be reported on at a later date. Measurements upon a number of commercially available instruments were reported, and in the following sections a discussion of the measurement methods is presented. The minimum amount of information needed to evaluate instrument performance is also discussed.

5.1 ULTRASONIC TRANSDUCER/SEARCH UNIT

The ultrasonic transducer or search unit is the most variable component of the ultrasonic test instrument. This variability results from the many different transducer designs, construction techniques, and materials used in transducer fabrication. The transducer is also susceptible to mechanical damage, wear, and deterioration due to aging. For this reason, search units should be evaluated and characterized as completely as is practical. This characterization should include an estimate of transducer 1) bandwidth or frequency response, 2) insertion loss or loop sensitivity, 3) a measure of the time domain response of the devices, 4) electrical impedance, and 5) sound field profiles.

Some measurement of efficiency is necessary for transducer evaluation. Either insertion loss or relative pulse echo sensitivity are adequate for this purpose. A loss of

efficiency is the clearest indication of transducer change or malfunction. The shape of an efficiency versus frequency plot is also helpful for determining if the faulty transducer has an electrical or a mechanical defect.

The time domain or impulse response of the transducer should be measured under well controlled and reproducible conditions. Single-cycle excitation from a 50-ohm signal generator or a transient pulse from a square wave pulser are well suited to this purpose. The use of a high-voltage pulser circuit from a standard ultrasonic test instrument, even though this is the pulse that will be used in an actual inspection, can lead to results which are difficult to interpret. This difficulty can be attributable to the variable and unknown properties of the pulser circuit.

Measurement of the transducer impedance is a relatively fast means for quickly screening transducers. This measurement can be accomplished using the transient methods described in this document or by using conventional RF impedance bridges. Ideally, the impedance of a transducer should be resistive over the frequency range of operation. Evaluation of transducer impedance is valuable because it can have a marked influence on the pulser and receiver performance. For example, it is difficult to drive a transducer if its impedance is substantially lower than the output impedance of the pulser.

The mapping of sound-field profiles for a transducer provides the definitive verification of the performance of an ultrasonic transducer. Such an evaluation allows beam shapes, focal properties, sidelobe levels, etc. to be measured directly rather than inferred.

5.2 RECEIVER-DISPLAY CHARACTERIZATION

The receiver frequency response and linearity for a limited number of instrument settings are presently being determined. The input sensitivity and noise are also recorded. All of these measurements are made with the instrument in the transmit/receive (pitch/catch) mode of operation. These measurements are all considered essential for receiver performance evaluation. Measurement of receiver-display linearity for a variety of instrument filter settings has revealed a number of receiver nonlinearities. It has also been noted that the chart recorder output of the receiver section does not identically track the video display of the echo amplitude. This condition is especially true for low-amplitude signals where it seems to be the source of instrument nonlinearity.

Other useful measurements have been identified but not yet implemented in this system. These measurements include: 1) frequency response and linearity in the pulse-echo mode, 2) input impedance, 3) dead time after transmit pulse saturation, and 4) dead time after echo saturation.

A good receiver-display section should have a center frequency which is well correlated with front panel settings. The bandpass should be sufficient to incorporate the frequency of the transducer. The instrument should be linear and its sensitivity should not be strongly affected by filter settings. Some degree of overlap in the bandpass for these different filter settings would allow the use of transducers with "nonstandard" operating frequencies.

5.3 PULSER

For characterization of the high-voltage pulser section of an ultrasonic instrument, it is necessary to measure either the time domain or frequency domain characteristics of

the output pulse. These measurements should be carried out with the pulser working into at least two known electrical loads. By comparing the response of the pulser working into two different loads, some insight is gained into the "effective" output impedance of the pulser circuit. This insight can be gained from either a time domain or a frequency domain measurement. Standard, linear circuit theory is inadequate for fully analyzing the output impedance of the high-voltage pulser because of the many nonlinear elements in the pulser circuit.

For maximum ultrasonic output from the transducer the "ideal" pulser circuit should have as low an output impedance as is practical. In addition, controls which influence the drive characteristics, such as pulse length, damping, and amplitude, should be designed to be recorded so that measurements can be reproduced at a later time.

REFERENCES

ASA (American Standards Association. 1970. American Standards C83.17 (also IEEE Stand. No. 177), American Standards Association, New York,

Burckhardt, C. B., H. Hoffman and P. A. Granchamp. 1973. "Ultrasound Axicon: A Device for Focusing Over a Large Depth." J. Acous. Soc. Am. 54:1628.

Carstensen, E. L. 1947. "Self-Reciprocity Calibration of Electroacoustic Transducers." J. Acous. Soc. Am. 19:961.

Erikson, K. R. 1974. "Tone-Burst Testin of Pulse-Echo Transducers." IEEE Trans. Sonics and Ultrasonics. SU-26:7.

Foldy, L. L. and H. Primakoff. 1947. "A General Theory of Passive Linear Electroacoustic Transducers and the Electroacoustic Reprocity Theorem. I." J. Acous. Soc. Am. 17:109.

Franlin, G. and T. Hatley. 1973. "Don't Eyeball Noise." Electronics Design. 24:184.

Gruchalla, M. E. 1980. "Measure Wide-Band White Noise Using a Standard Oscilloscope." Electronic Design News, 157.

MacLe[illegible], W. R. 1940. "Absolute Measurement of Sound Without a Pri[illegible]ary Standard." J. Acous. Soc. Am. 12:140.

O'Donnell, M., L. J. Busse and J. G. Miller. 1981. "Piezoelectric Transducers." In Methods of Experimental Physics, P. D. Edmund, ed., Vol. 19, pp. 29-65, Academic Press. New York, New York.

Papadakis, E. P. 1977. "Ultrasonic Transducer Evaluation in Five 'Domains': Time, Space, Frequency, Surface Motion, and Theory." Ultrasonics Symposium Proceedings, Cat. #77 CH1264-1 SU, IEEE.

Posakony, G. J. 1975. "Engineering Aspects of Ultrasonic Piezoelectric Transducer Design." Ultrasonics Symposium Proceedings, Cat. #75 CHO 994-4SU, IEEE.

Primakoff, H. and L. L. Foldy. 1947. "A General Theory of Passive Linear Electroacoustic Transducers and the Electroacoustic Reciprocity Theorem. II." J. Acous. Soc. Am. 19:50.

Reid, J. M. 1974. "Self-Reciprocity Calibration of Echo-Ranging Transducers." J. Acous. Soc. Am. 55:862.

Sabin, G. A. 1964. "Calibration of Piston Transducers at Marginal Test Distances." J. Acous. Soc. Am. 36:168.

Sachse, W. "On the Reversibility of Piezoelectric Transducers." MSC Report 2926, Cornell University, Ithaca, New York.

Sachse, W. and N. N. Hsu. 1979. "Ultrasonic Transducer for Materials Testing and Their Characterization." In Physical Acoustics, XIV. W. P. Mason and R. N. Thurston, eds., Academic Press, New York, New York.

Sittig, E. K. 1967. "Transmission Parameters of Thickness-Driven Piezoelectric Transducers Arranged in Multilayer Configuration," IEEE Trans. Sonics and Ultrasonics, SU-14:167.

Volterra, V. 1959. Theory of Functionals and of Integral and Integro-Differential Equations. Dover, New York, New York.

Weiner, D. D. and J. E. Spina. 1980. Sinusoidal Analysis and Modeling of Weakly Nonlinear Circuits. Van Nostand, New York, New York.

Wuestenberg, H. 1970. "Contactless Electrodynamic Ultrasonic Transducers and Their Application in Ultrasonic Inspection." B-4. In Proceedings of the Sixth International Conference on NDT, Hanover, Germany.

Wuestenberg, H., E. Mundry, W. Moehrle and W. Wegner. 1979. "Experiences with the Use of Electrodynamic Microprobes for Probe Characterization." 4H-6. In Proceedings of the Ninth World Conference on NDT.

DISTRIBUTION

No. of Copies

OFFSITE

U.S. Nuclear Regulatory Commission
Division of Reactor Safety Research
7920 Norfolk Avenue
Bethesda, MD 20014

400 U.S. Nuclear Regulatory Commission
Division of Technical Information and Document Control
7920 Norfolk Avenue
Bethesda, MD 20014

M. R. Hum
U.S. Nuclear Regulatory Commission
Materials Engineering Branch
Mail Stop 318
Washington, DC 20555

Stewart D. Ebneter
USG Nuclear Regulatory Commission
1075 Brentwood Dr.
Pottstown, PA 19464

2 DOE Technical Information Center

Robert R. Arant
125 Seriff Dr.
Lima, OH 45807

Larry J. Chockie
6729 Landerwood Lane
San Jose, Calif 95120

No. of Copies

70 Ralph G. Crawford
270 Inglewood Dr.
Pittsburgh, PA 15228

David E. Dier
73 Wildwood Dr.
Barrington, IL 60010

Solomon Goldspiel
732 Gerald Court
Brooklyn, NY 11235

Joseph D. Marble
69 Handel Lane
Cincinnati, OH 45218

Warren H. Mayo
40 Newgate Road
Pittsburgh, PA 15202

Henry D. Monsch
1652 South Abrego Dr.
Green Valley, AZ 85614

Bernard Ostrofsky
P.O. Box C
Naperville, IL 60566

Harold L. Pinsch
4117 Phinney Bay Dr.
Bremerton, WA 98310

No. of
Copies

Robert J. Roehrs
4762 Barroyal Dr.
St. Louis, MO 63128

Walter N. Roy
302 Potter Road
Framingham, MA 01701

John G. Rumbold
1014 Whitehead Road Ext.
Trenton, NJ 08638

F. J. Sattler
873 Old Spring Road
Copley, OH 44321

Alan Schoffman
592 Warwick Avenue
Teaneck, NJ 07666

Michael L. Stellabotte
384 Westfield Dr.
Broomall, PA 19008

William A. Sverkric
5200 Arrowood Ct.
Columbus, OH 43229

Carlos F. Morcate
ACF Industries
W K M Valve Div.
Box 2117
Houston, TX 77001

Don L. Conn
ARMCO Inc.
Research Center
Middletown, OH 45043

Paul T. Duffey
Al Tech Specialty Steel
Corp.
Spring St. Road
Watervliet, NY 12189

Thomas F. Drumwright, Jr.
Alcoa Technical Center
Alcoa Center, PA 15069

No. of
Copies

Jack B. Morgan
Allegheny Ludlum Industries
Inc.
Research Center
Brackenridge, PA 15014

John Winslow Newman
Allied Piping Prod. Co.
2550 Blvd. of the Generals
Norristown, PA 19403

Moss V. Davis, Dr.
American Welding Soc., Inc.
Box 351040-550 NW Le Jeune
Miami, FL 33135

Carl Russell
Aquatic Professionals, Inc.
5151 Michelldale A-5
Houston, TX 77092

Arnold H. Greene
Arnold Greene Testing
Labs, Inc.
6 Huron Drive
Natick, MA 01760

Howard E. Van Valkenbu
Automation Industries, Inc.
P.O. Box 3500
Danbury, CT 06810

H. C. Graber
Babcock & Wilcox
91 Sterling Avenue
M/S BW041B
Barberton, OH 44203

Harold C. Graber
Babcock & Wilcox
4-1-48
91 Stirling Ave.
Barberton, OH 44203

M. G. Hacker
Babcock & Wilcox
Nuclear Power Generation Dept.
P.O. Box 239
Lynchburg, VA 24505

No. of
Copies

A. Holt
Babcock & Wilcox
91 Sterline Avenue
Barberton, OH 44203

W. E. Lawrie
Babcock & Wilcox
P.O. Box 1260
Lynchburg, VA 24505

William E. Lawrie
Babcock & Wilcox
Lynchburg Research Center
P.O. Box 239
Lynchburg, VA 24505

B. L. Laubert
Babcock & Wilcox
Tubular Products Division
640 E. Keystone St.
Alliance, OH 44601

Maryellen Robards
Bardel, Inc.
13810 Enterprise Ave.
Cleveland, OH 44135

G. Joseph Wolf
Bethlehem Steel Corp.
Room 341 GSO
Bethlehem, PA 18016

Wayne J. Ferguson, II
Black-Civalls & Bryson
4011 E. 67th St.
Tulsa, OK 74136

Samuel Greenberg
Bldg. 142 - Apt. 207
9861 Sunrise Lakes Blvd.
Sunrise Ft. Laude., FL 33322

Carl H. Himmelman
Borg-Warner Corp.
Byron Jackson Pump Division
5800 S. Eastern Ave.
Commerce, CA 90040

No. of
Copies

William C. Lowenkamp
Box 878 - Monticello Road
Hazlehurst, MS 39083

Paul J. Bulten
Brown & Root Inc.
6021 Bonhomme-Crest Park
Bldg.
Houston, TX 77036

Ronald C. Bevan
CBL Industries Inc.
13810 Enterprise Avenue
Cleveland, OH 44135

Vincent L. Gorka
Carpenter Technology Corp.
133 Springfield Road
Union, NJ 07083

Richard B. Moyer
Carpenter Technology Corp.
101 W. Bern St.
Reading, PA 19603

F. C. Berry
Chicago Bridge & Iron
P.O. Box 277
Burmingham, AL 35201

J. L. Wood
Combustins Power Co.
1945 Parnall Road
Jackson, MI 49201

O. F. Hedden
Combustion Engineering
Dept. 9004-2228
1000 Prospect Hill Road
Windsor, CT 06095

E. J Parent
Combustion Engineering
Dept. 9451-201
Windsor, CT 06095

No. of
Copies

T. L. Bailey
Combustion Engineering Inc.
FPSM Quality Assurance
911 W. Main St
Chattanooga, TN 37401

Donald L. Crabtree
Comustion Engineering, Inc.
911 W. Main St.
Chattanooga, TN 37402

Howard B. Aaron
D A B Industries Inc.
Vice President Engrg. & Res.
466 Stephenson Highway
Troy, MI 48084

Rudolf W. Zillmann, Dr
DCASR-Cleveland DCRO-QT.
1240 E. 9th St.
Cleveland, OH 44199

A. A. Churm
DOE Patent Division
9800 S. Cass Avenue
Argonne, IL 60439

W. J. McGonnagle
DOE/NBL
9800 S. Cass Avenue
Argonne, IL 60439

J. F. Cook
EG&G Idaho, Inc.
P.O. Box 1625
Idaho Falls, ID 83401

D. E. McDonald
EPRI NDE Center
P.O. Box 217097
Charlotte, NC 28221

John R. Zimmerman
East Texas State University
College of Sciences & Tech.
East Texas Station
Commerce, TX 75428

No. of
Copies

John Waskow
Eastman Kodak Co.
Kodak Park Div. Bldg. 23
Rochester, NY 14650

Gary Dau
Electric Power Research Inst.
P.O. Box 10412
Palo Alto, CA 94303

Kirit V. Smart
Florida Power & Light Co.
Plant Construction Dept.
400 N. Congress Ave.
P.O. Drawer D
West Palm Beach, FL 33402

Emmanuel P. Papadakis
Ford Motor Co.
Mfg. Dev. Center
621 Henley Dr.
Birmingham, MI 48008

Gordon R. Woodrow
G.O. Carlson Inc.
Marshalltown Road
Thorndale, PA 19372

L. J. Chockie
General Electric
M/C 363
175 Curtner Avenue
San Jose, CA 95125

B. R. Rajala
General Electric
175 Curtner Avenue
M/C 273
San Jose, CA 95125

Gilbert E. Joly
General Electric Co.
1 River Road, Bldg. 28-450
Schenectady, NY 12345

Derek J. Sturges
General Electric Co.
Interstate Hwy 75-Bldg. 700-E45
Cincinnati, OH 45215

No. of
Copies

C. D. Cowfer
General Public Utilities
100 Interpace Parkway
Parsippany, NJ 07054

V. H. Hight
Gilbert Associates
P.O. Box 1498
Reading, PA 19603

Bernard M. Strauss
Gulf Science & Technology Co.
P.O. Drawer 2038
Pittsburgh, PA 15230

D. R. Allan
Guterl Special Steel Corp.
P.O. Box 509
Ohio Street
Lockport, NY 14094

Robert Goldstein
Guterl Special Steel Corp
Ohio St.
P.O. Box 509
Lockport, NY 14094

Robert V. Harris
Harisonic Labs Inc.
7 Hyde Street
Stamford, CT 06902

F. T. Duba
Hartford Steam Boiler
Inspection and Insurance
Company 56 Prospect Street
Hartford, CT 06102

Dennis Allen White
Hartford Steam Boiler
Inspection and Insurance
8 Colburn Road
Stafford Springs, CT 06076

Ted Kirk
Huntington Alloys Inc.
P.O. Box 1958
Huntington, WV 25720

No. of
Copies

Daniel F. McGrath
Ingersoll-Rand Oil Field
Products Co.
P.O. Box 1101
Pampa, TX 79065

Frank E. Faris
Interdevelopment, Inc.
Rutherford B. Hayes Bldg.
2361 Jeff Davis Hwy - STE 1014
Arlington, VA 22202

Jesse W. Caum
International Center for
Diffraction Data
1601 Park Lane
Swarthmore, PA 19081

Virgil B. Roberts
International Nickel
Huntington Alloys Inc.
Guyan River Road Box 1958
Huntington, WV 25720

F. L. Becker
J. A. Jones Applied Research Co.
1300 Harris Blvd.
P.O. Box 217097
Charlotte, NC 28221

R. M. Stone
J. A. Jones Applied Research Co.
1300 Harris Blvd.
P.O. Box 217097
Charlotte, NC 28221

Robert S Spinetti
Jones & Laughlin Steel Corp.
Works Testing Lab
P.O. Box 490
Aliquippa, PA 15001

Jeffrey A. Bailey
Kaiser Aluminum & Chemical
Box 877 - 6177 Sunol Blvd.
Pleasanton, CA 94566

No. of
Copies

Robert B. Wilson
Kennametal Inc.
1 Lloyd Avenue
Box 231
Latrobe, PA 15650

John E. Bobbin
Krautkramer Branson
International
250 Long Beach Blvd Box 408
Stratford, CT 06497

Theodore G. Lambert
Lambert Mac Gill Thomas, Inc.
771 E. Brokaw Road
San Jose, CA 95112

George V. Aseff, Sr.
Law Engineer Testing Co.
396 Plasters Ave. NE
Atlanta, GA 30324

Edward Karapetian
Los Angeles City Of.
Dept. of Water & Power-Room 1023
Box 111
Los Angeles, CA 90051

John P. Sunukjian
Lukens Steel Co.
No. 2421
Coatesville, PA 19320

E. B. Lewis
Lynchburg Foundry Co.
NDT-Research & Development
P.O. Drawer 411
Lynchburg, VA 24505

Robert A. Hanson
MPB Corporation
P.O. Box 547
Keene, NH 03431

Matthew J. Dashukewich
Magnaflux Corp.
230 Murphy Road
Hartford, CT 06114

No. of
Copies

Peter J. Suhr
Magnetic Analysis Corp.
535 S. Fourth Avenue
Mt. Vernon, NY 10550

B. Boro Djordjevic
Martin Marietta Labs.
1450 S. Rolling Road
Baltimore, MD 21227

Richard J. Meyer
McDonnell Douglas Corp.
Dept. 8528 - Bldg. 220
P.O. Box 516
St. Louis, MO 63166

Mr. Connie Presley
Mid Continent Steel Casting
Div. of Kast Metals
Box 6611M
Shreveport, LA 71106

Richard S. Humphrey
Monsanto Co.
800 N. Lindbergh Blvd F4EE
St. Louis, MO 63166

Claude E. Jaycox
Municipal Testing Lab. Inc.
160 Lauman Lane
Hicksville, NY 11801

Charles H. Craig
Naval Sea Systems Command
Sea 05E2
Washington, DC 20362

Clifford W. Anderson
Naval Surface Weapons Center
Code R34
White Oak
Silver Spring, MD 20910

Giancarlo Mazzoleni
Newage Industries, Inc.
2300 Maryland Road
Willow Grove, PA 19080

No. of
Copies

Robert R. Hardison
Newport News Shipbuilding &
Drydock CC - Dept. 035
4100 Washington Ave.
Newport News, VA 23607

E. Debarba
Northeast Utilities
P.O. Box 270
Hartford, CT 06101

P. S. Barry
Nuclear Energy Services Inc.
NES Div.
Shelter Rock Road
Danburg, CT 06810

John H. Weiler
Offshore Power Systems
8000 Arlington X-Way
Jacksonville, FL 32211

Kenneth P. Weaver
Ohio Steel Tube Co.
West Main St.
Shelby, OH 44875

Robert Smetana
Orbit Industries, Inc.
6840 Lake Abram Dr.
Middleburg Hts, OH 44130

Richard I. Buckley
P.O. Box 941
Attleboro, MA 02703

James D. Nordstrom
PA Incorporated
P.O. Box 7631
Houston, TX 77007

F. J. Dodd
Pacific Gas and Electric Co.
77 Beal Street, Rm 2411
San Francisco, CA 94106

No. of
Copies

Frederick H. C. Hotchkiss
Panametrics, Inc.
221 Crescent Street
Waltham, MA 02154

College of Textile Science
Pastore Philadelphia Library
3243 School Lane
Philadelphia, PA 19144

P. J. Herbert
Paul J. Herbert, Inc.
212 Paseo Del Rio
Moraga, CA 94556

Carl B. Shaw
Portland General Electric Co.
Generation Engrg. S B Bridge
121 SW Salmon St.
Portland, OR 97204

C. R. Felmley, Jr.
Executive Secretary
Pressure Vessel Research
Committee Welding Research Council
345 E. 47th Street
New York, NY 10017

Noel B. Proctor
Proctor Inspection
Consultants Inc.
1507 Brooks
Rosenberg, TX 77471

Roger P. Maickel, Dr.
Purdue University - Dept. of
Pharmacology & Toxicology
School of Pharmacal Sci.
W. Lafaette, IN 47907

James H. Bly
Radiation Dynamics, Inc.
56 Fieldstone Drive
Syosset, NY 11791

No. of
Copies

Neil W. Breslow
Radiatronics NDT, INC
P.O. Box 12308
Overland Park, KS 66212

J. Harvey Wynne
Republic Steel Corp.
1570 Glenhardie Road
Wayne, PA 19087

Richard Gaydos
Republic Steel Corp.
Tech Services
P.O. Box 6778
Cleveland, OH 44101

Carlton E. Burley
Reynolds Metals Co.
Box 27003
Richmond, VA 23261

Warren L. Mehnert
Sandusky Foundry & Machine Co.
615 W. Market St.
Sandusky, OH 44870

Jerry T. McElroy
Search Unit Systems Inc.
12918 Bandera Road
San Antonio, TX 78228

Jack W. Raisch
Sonic Instruments, Inc.
1014 Whitehead Road Ext.
Trenton, NJ 08638

Roy Gromlich
Sonic Instruments Inc.
1018 Whitehead Road
Trenton, NJ 08638

W. T. Clayton
Southwest Research Inst.
6220 Culebra Road
P.O. Drawer 28510
San Antonio, TN 78284

No. of
Copies

W. T. Flach
Southwest Research Inst.
6220 Culebra road
P.O. Drawer 28510
San Antonio, TX 78284

William C. Mc Gaughey
Southwest Research Institute
P.O. Drawer 28510
San Antonio, TX 78284

Wayne W. Rogers
Standard Precision Inc.
12311 S. Shoemaker Avenue
Sante Fe Springs, CA 90670

James D. Bean
Superior Tube Co.
Box 191
Norristown, PA 19404

Cohen Yoseph Bar
Systems Research Labs Inc.
2800 Indian Ripple Road
Dayton, OH 45440

Parviz Mahmoodi
3M Company
Central Res. 201-BE
P.O. Box 33221
St. Paul, MN 55133

Floyd A. Brown
Titanium Metals Corp.
100 Titanium Way
Toronto, OH 43964

Edwin B. Henry, Jr.
U.S. Steel Research Laboratory
125 Jamison Lane
Monroeville, PA 15146

Bernard Strauss
USA Watertown
Army Mats. & Mech. Res. Ctr.
Arsenal St
Watertown, MA 02160

No. of
Copies

Patrick C. McEleney
USA Watertown Materials &
Mechanics Research Center
Arsenal Street
Watertown, MA 02172

Charles Federman
USG Commerce
National Bureau of Stds.
Bldg. 233 - Room A147
Washington, DC 20234

Donald G. Eitzen
USG Commerce
National Bureau of Stds.
Sound A147
Washington, DC 20234

Daniel J. Chwirut
USG HHS - Silver Spring
FDA-Bureau of Medical Devices
8757 Georgia Ave.
Silver Spring, MD 20910

Stewart D. Ebneter
USG Nuclear Regulatory
Commission
1075 Brentwood Dr.
Pottstown, PA 19464

John Mittleman
USN Naval Coastal Systems Lab.
Panama City, FL 32407

Stephen D. Hart
USN Naval Research Lab.
4555 Overlook Ave. SW Code 8435
Washington, DC 20375

Edward L. Criscuolo
USN Naval Weapons Center
White Oak Lab-Code R34
Silver Spring, MD 20910

No. of
Copies

Kenneth Von Cook
Union Carbide Corp.
Oak Ridge National Lab
P.O. Box X Bldg. 4500S
Oak Ridge, TN 37830

Robert W. Mc Clung
Union Carbide Corp.
Oak Ridge Natl. Lab.
P.O. Box X
Oak Ridge, TN 37830

Douglas L. Marriott
University of Illinois
1206 W. Green
Urbana, IL 61801

Steven Serabian
University of Lowell
Mechanical Engineering Dept.
North Campus
Lowell, MS 01854

Kermit A. Skeie
Uresco
10603 Midway Ave.
Cerritos, CA 90701

Edmund G. Henneke
VA Polytechnic Inst. & State U.
Dept. of Engineering Science and
Mechanics
Blacksburg, VA 24061

John D. Fenton
Vought Corporation
P.O. Box 225907 MZ 6-16
Dallas, TX 75265

A. L. Smith
Washington Public Power
Supply System
P.O. Box 968
Mail Drop 675
Richland, WA 99352

No. of
Copies

Chuck Taylor
Western Zirconium
P.O. Box 3208
Odgen, UT 84409

Eugene T. Hughes
Westinghouse Electric
Water Reactors Div.
Mat'ls & NDE Analysis Box 355
Pittsburgh, PA 15230

E. T. Hughes
Westinghouse Electric Co.
P.O. Box 355
Pittsburgh, PA 15230

D. C. Adamonis
Westinghouse Electric Corp.
Nuclear Technology Division
P.O. Box 355
Pittsburgh, PA 15230

Dominick J. De Paul
Westinghouse Electric Corp.
Box 425
Monroeville, PA 15146

Calvin W. Mc Kee
Westinghouse Electric Corp.
P.O. Box 9175
Mail Code N107
Lester, PA 19113

David R. McLemore
Westinghouse Hanford Co.
WA-22
Box 1970
Richland, WA 99352

Mike C. Tsao
Westinghouse R&D
1310 Beulah Road
Pittsburgh, PA 15235

No. of
Copies

Robert W. Loveless
Worthington Group
McGraw-Edison Co.
401 Worthington Avenue
Harrison, NJ 07029

Robert A. Eddy
Wyman-Gordon Co.
Worcester St
North Grafton, MA 01536

J. J. Lance
Yankee Atomic Electric Co.
1671 Worcester Road
Framingham, MA 01701

J. C. Spanner
Spanner Engineering Inc.
c/o Bestco
2939 Park Drive
P.O. Box 1370
Richland, WA 99352

FOREIGN

Lars-Ake Kornvik
A B Statens Anloggningsprovning
Kemistvagen 21, Box 51
S-183 21 TABY
SWEDEN

Don Birchon
Admiralty Materials Laboratory
Holton Health Poole
Dorser, ENGLAND
020-122-2711

No. of
Copies

John Geoffrey Harris
Alcan Plate LTD
P.O. Box 383
Kitts Green RD B33 9QR
Birmingham
ENGLAND

David C. Broom
Aluminum Co. of Canada Ltd.
Research Center
P.O. Box 8400 - Kingston
Ontario K7L 4Z4 CANADA

Mervyn Brown
Aspex Services
214 Main Street East
Milton Ontario L9T 1N8
CANADA

ACE Sinclair
Berkeley Nuclear Laboratories
Research Division
Berkeley
Gloucestershire, CL 13 9 PB
U.K.

E. E. Borloo
Commission of the European
Communities
Joint Research Center
21020 ISPRA (VA)
ITALY

J. A. De Raad
Delftweg 144
3046 NC Rotterdam
NETHERLANDS

O. Forli
Det Norske Veritas
Veritasveien, 1
P.O. Box 300
N-1322 Hovik
NORWAY

No. of
Copies

Herbert Schaim
I M D T (Industrial &
Scientific Equipment)
9 Keren Ha'Yesod St P O B 1155
Beer-Sheva ISRAEL

P. Holler
Institut fur Zerstrarangs Frere
Prufverfahren
Univ. Geb. 37
D-6600 Saarbrucken
WEST GERMANY

M. J. Whittle
NDT Application Centre
C.E.G.B. Scientific Services
Timpson Road
Manchester M23 9LL
U.K.

O. A. Kupcis
Ontario Hydro
Tortonto, Ontario M8Z 5S4
CANADA

I. P. Bell
Risley Nuclear Labs
UKAEA
Risley Warrington
Cheshive
U.K.

X. Edelman
Sulzer Brothers Ltd.
Dept. 1513, NDT
CH-8401 Winterthur
SWITZERLAND

P. Caussin
vincotte
1640 Rhode-Saint-Genese
BELGIUM

Horacio Prevedel
2577 Salgvero Street
Buenos Aires 1425
ARGENTINA

No. of
Copies

ONSITE

50 Pacific Northwest Laboratory

A. S. Birks
S. H. Bush
L. J. Busse
R. A. Clark
S. R. Doctor (32)
G. B. Dudder
P. G. Heasler
P. H. Hutton
G. J. Posakony
G. P. Selby
F. A. Simonen
A. M. Sutey
T. T. Taylor
Technical Information (5)
Publishing Coordination (2)

NRC FORM 335 (11-81)

U.S. NUCLEAR REGULATORY COMMISSION

BIBLIOGRAPHIC DATA SHEET

1. REPORT NUMBER *(Assigned by DDC)*
NUREG/CR-2264
PNL-4215

4. TITLE AND SUBTITLE *(Add Volume No., if appropriate)*
Characterization Methods for Ultrasonic Test Systems

2. *(Leave blank)*

3. RECIPIENT'S ACCESSION NO.

7. AUTHOR(S)
L.J. Busse, F.L. Becker, R.E. Bowey, S.R. Doctor, R.P. Gribble, G.J. Posakony

5. DATE REPORT COMPLETED
MONTH: April YEAR: 1982

9. PERFORMING ORGANIZATION NAME AND MAILING ADDRESS *(Include Zip Code)*
Pacific Northwest Laboratory
Richland, WA 99352

DATE REPORT ISSUED
MONTH: July YEAR: 1982

6. *(Leave blank)*

8. *(Leave blank)*

12. SPONSORING ORGANIZATION NAME AND MAILING ADDRESS *(Include Zip Code)*
Division of Engineering Technology
Office of Nuclear Regulatory Research
U.S. Nuclear Regulatory Commission
Washington, DC 20555

10. PROJECT/TASK/WORK UNIT NO.

11. FIN NO.
B2289

13. TYPE OF REPORT

PERIOD COVERED *(Inclusive dates)*

15. SUPPLEMENTARY NOTES

14. *(Leave blank)*

16. ABSTRACT *(200 words or less)*

Methods for the characterization of ultrasonic transducers (search units) and instruments are presented. The instrument system is considered as three separate components consisting of a transducer, a receiver-display, and a pulser. The operation of each component is assessed independently. The methods presented were chosen because they provide the greatest amount of information about component operation and were not chosen based upon such conditions as cost, ease of operation, field implementation, etc. The results of evaluating a number of commercially available ultrasonic test instruments are presented.

17. KEY WORDS AND DOCUMENT ANALYSIS

17a. DESCRIPTORS

17b. IDENTIFIERS/OPEN-ENDED TERMS

18. AVAILABILITY STATEMENT
Unlimited

19. SECURITY CLASS *(This report)*
Unclassified

21. NO. OF PAGES

20. SECURITY CLASS *(This page)*
Unclassified

22. PRICE
$